RAT LIVER FERRITIN
BIOCHEMICAL AND MICROANALYTICAL ASPECTS

Rattelever ferritine
Biochemische en microanalytische aspecten

Proefschrift

ter verkrijging van de graad van doctor
aan de Erasmus Universiteit Rotterdam
op gezag van de Rector Magnificus
Prof. dr. C.J. Rijnvos
en volgens besluit van het College van Dekanen.
De openbare verdediging zal plaatsvinden op
woensdag 18 september 1991 om 15.45 uur

door

Patricia Louise Ringeling
geboren te Amsterdam

universiteits
DRUKKERIJ
1991

Promotie-commissie

Promotor:	Prof. dr. H.G. van Eijk
Overige leden:	Prof. dr. K. van Dam
	Prof. dr. J.F. Koster
	Prof. J.H.P. Wilson

Van de maan af gezien zijn
we allemaal even groot

Multatuli

voor Norma

Het onderzoek dat leidde tot de totstandkoming van dit proefschrift kon alleen worden uitgevoerd dankzij de steun en inzet van de medewerkers van de afdelingen
Chemische Pathologie en Pathologische Anatomie, AEM unit
van de Erasmus Universiteit Rotterdam

Linguistic support: A. Miller

CONTENTS page

LIST OF ABBREVIATIONS

BSA	bovine serum albumin
CF	cytosolic ferritin
CLF	cytosolic light ferritin
CMF	cytosolic monomeric ferritin
CTEM	conventional transmission electron microscopy
CVVF	cytosolic void volume ferritin
DNase	deoxyribonuclease
DMSO	dimethyl sulphoxide
E	energy
ΔE	energy loss
EBSS	Earl's balanced salt solution
EDTA	ethylenediaminetetraacetic acid
EELS	electron energy-loss spectroscopy
EPMA	electron probe microanalysis
ESI	electron spectroscopic imaging
Gal	galactose
GlcNAc	*N*-acetylglucosamine
h	hour(s)
Hepes	*N*-2-hydroxyethylpiperazine-*N'*-2-ethanesulfonic acid
HS	haemosiderin
IE	ionization edge
IEF	isoelectric focusing
kDa	kilodalton(s)
LDH	lactate dehydrogenase
LF	lysosomal ferritin
LLF	lysosomal light ferritin
Man	mannose
MIC	mean iron-content
min	minute(s)
mRNA	messenger ribonucleic acid

NADH	nicotinamide adenine dinucleotide, reduced form
NANA	*N*-acetylneuraminic acid (sialic acid)
Nleu	norleucine
PAGE	polyacrylamide gel electrophoresis
p*I*	isoelectric point
PIE	pre-ionization edge
PMSF	phenylmethanesulphonyl fluoride
p-TSA	toluene-4-sulphonic acid
ROI	region(s) of interest
SD	standard deviation
SDS	sodium lauryl sulphate
sec	second(s)
SF	siderosomal ferritin
SIC	siderosomal iron compound
SVVF	siderosomal void volume ferritin
Tris	tris(hydroxymethyl)aminomethane
vol	volume(s)
v/v	volume/volume
v/w	volume/weight
w/w	weight/weight

CHAPTER 1

GENERAL INTRODUCTION

This thesis is an investigation into the relationship between ferritin and haemosiderin, the major compounds in haemochromatosis, a genetic disorder leading to a severe disturbance of iron metabolism. In this study ferritins and ferritin-related compounds present in the livers of experimentally iron-loaded rats are analysed and compared, with each other and with haemosiderin. The results of this study will be preceded by a summary of iron metabolism.

Iron in the human body

Iron plays a critical role in many biological processes in the human body. Bound to protoporphyrin it forms the prosthetic group in haem proteins, which are involved in the neutralization (cytochromes, peroxidase and catalase) and transport (haemoglobin and myoglobin) of oxygen. Iron itself is mainly transported through the body by the plasma protein transferrin and excess iron is stored in ferritin and haemosiderin. The distribution of iron among various compartments of the human body is shown in Figure 1.1. Normally, iron uptake (from ingested food) and iron loss (through blood loss and perspiration) are in balance. This balance can only be maintained by adapting iron uptake to iron loss, because there is no known active iron excretion mechanism.

Iron intake and absorption

As iron is only poorly absorbed, the diet has to contain relatively large amounts of it to meet requirements. Haem iron, which is only found in meat, is more readily absorbed than non-haem iron. The latter can only be absorbed from the intestinal lumen in the Fe(II) state. The acidic environment of the stomach and reducing agents present in the food (e.g. vitamin C) can reduce Fe(III) to Fe(II) and thus promote the dietary uptake of iron. Other food constituents (e.g. tannins in tea), inhibit the uptake by forming insoluble compounds with iron [1]. Once absorbed by the mucosal cells of the duodenum, iron is

transported to the bloodstream. The amount of iron transported is regulated by an unknown mechanism and is dependent on how much iron is needed by the body.

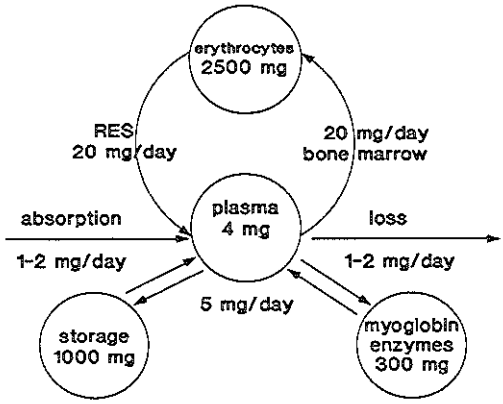

Figure 1.1
Distribution of iron in the human body and exchange between various compartments.

Iron transport

Most non-haem iron is transported through the body by the plasma protein transferrin. Transferrin is a glycoprotein of about 80 kDa, which is synthesized in the liver. It consists of a single polypeptide chain with two iron binding domains, the N-terminal domain and the C-terminal domain. *In vitro*, each domain can bind one ferric atom, but they differ in their affinity for it, depending on the pH and ionic composition of the medium. In the C-terminal domain two branched carbohydrate units are present. One of the sugar residues present in these units is the negatively charged *N*-acetylneuraminic acid

(sialic acid). Microheterogeneity of transferrin is caused by variations in the degree of branching of the carbohydrate units and in the number of sialic acid residues present in these units (Figure 1.2).

When a cell needs iron, it expresses transferrin receptors at its surface. Transferrin molecules (with iron) bind to transferrin receptors and are internalized by receptor-mediated endocytosis. Intracellularly, acidic endosomes are formed in which iron is uncoupled from the transferrin molecule, which is still bound to its receptor. While the iron is used in the cell for biological processes or stored in intracellular ferritin, the transferrin/transferrin-receptor complex is recycled to the cell membrane. Here, the transferrin molecule is uncoupled from its receptor and is once again able to bind extracellular iron (for review see [2]).

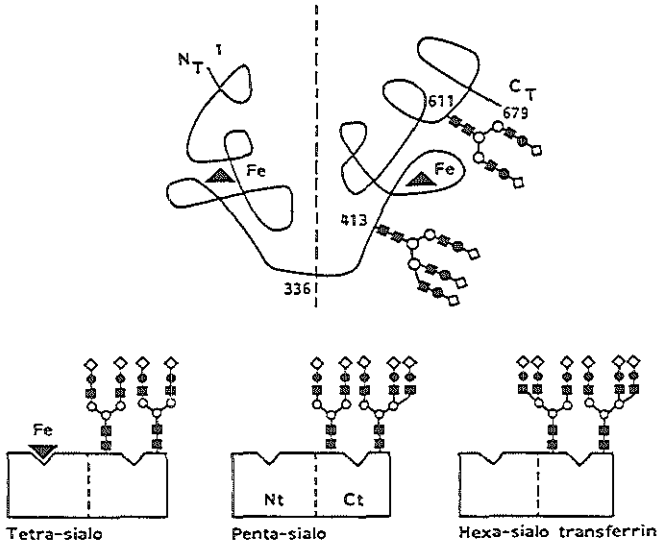

Figure 1.2

Schematic representation of the transferrin molecule. The broken line indicates the division between the two globular domains. Three microheterogeneous forms of human transferrin are shown at the bottom of the figure. ■*=GlcNAc,* ○*=Man,* ●*=Gal,* ◇*=NANA (from [2]).*

Iron storage

Ferritin

Ferritin is the primary iron storage compound of the human body under normal circumstances (for review see [3]). It is found in several tissues and consists of an iron-containing core, approximately 6 nm in diameter, in which iron is present as a polynuclear ferric oxyhydroxide-phosphate complex. The iron core is surrounded by a protein coat.

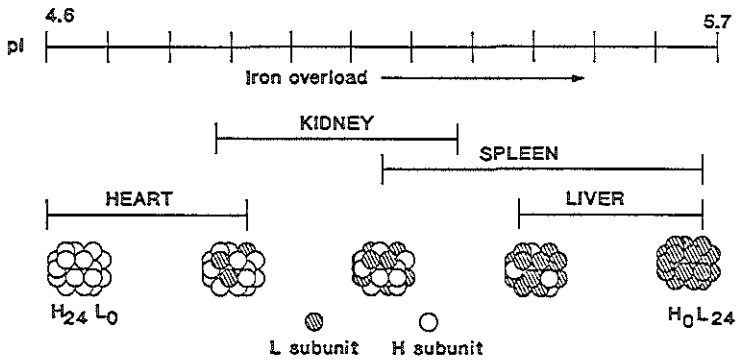

Figure 1.3
The range of isoferritins.

This coat, a complex of 24 polypeptide subunits, keeps iron in a soluble and non-toxic form. There are two types of subunit: heavy (H) and light (L) subunits, the former having eight extra amino acids. Microheterogeneity of ferritin is the result of different combinations of these subunits, ranging from $H_{24}L_0$ to H_0L_{24} (Figure 1.3). Heart ferritins consist predominantly of H subunits, whereas liver and spleen ferritins consist predominantly of L subunits. H and L subunits may have functional differences. It has been suggested that H rich ferritins, which usually have a low iron content, are metabolic

ferritins, whereas the ferritins which are rich in L subunits, which usually have a high iron content, are in fact storage ferritins [4].

As a reaction to an iron stimulus H and L subunit mRNAs, already present in the cytosol as inactive ribonucleoprotein particles, are translated on free ribosomes. Recent studies indicate that iron stimulates cytoplasmic proteins to bind to a highly-conserved sequence in the 5' untranslated region of H and L subunit mRNAs [5,6].

The subunits are assembled in such a way that an apoferritin molecule with 14 channels is created. Through these channels iron, in the form of Fe(II), can enter the core. In the process of entering the core, Fe(II) is oxidized to Fe(III). It has been suggested that the ferroxidase centre is exclusively located on H subunits [7,8]. Both partially filled ferritins and newly-assembled apoferritins can take up iron. Although there is place for about 4500 iron atoms in the core, the average number found is 2500, even under iron-overload conditions. Differences in iron content explain ferritin heterogeneity.

Apart from iron the ferritin core contains phosphorus, oxygen and hydrogen. The iron core of ferritin from horse spleen - a very rich source of ferritin - can be represented by $(FeOOH)_8(FeO\text{-}OPO_3H_2)$ [9]. The cores of ferritins from other sources are generally assumed to be similar. The amount of phosphorus present in the core varies from individual to individual and from tissue to tissue [10,11]. It is not clear at what stage phosphorus and oxygen are incorporated.

Under iron-overload conditions there is an increase in L-mRNA level [12] resulting in more L subunits and L-rich ferritins. It has been suggested that the increase is the result of the stabilization of L-mRNA transcripts by the action of a cytosolic protein [13]. As L subunits are more basic than H subunits, under iron-overload conditions there is a shift towards a higher isoelectric point.

Small amounts of ferritin are present in serum [14]. In contrast to intracellular ferritin, serum ferritin is glycosylated. Under normal circumstances the serum ferritin concentration is very low, but in cases of iron overload the concentration increases.

Haemosiderin

Less is known about haemosiderin (for review see [15]). It is found in later stages of iron overload in iron rich lysosomes, also called siderosomes, next to ferritin.
Haemosiderin ultrastructurally resembles ferritin. The main difference between ferritin and haemosiderin is that the latter is water-insoluble, probably due to the lack of an intact protein coat. It consists of iron-containing granules visible under the electron microscope as irregular massive aggregates of electron dense particles resembling ferritin iron cores. The particles are of irregular shape with diameters ranging from 1 to 7.5 nm.

Relationship between ferritin and haemosiderin

Since ferritin and haemosiderin have similar X-ray diffraction patterns [16], Mössbauer spectra [17] and peptides [18], it is generally assumed that haemosiderin is a degradation product of ferritin. The exact transition mechanism, however, is still unclear. One theory [19] maintains that changes at the surface of ferritin molecules could be a signal for polymerization, and this a signal for incorporation into lysosomes. Another theory [20] suggests that decomposition of the protein shell of ferritin in lysosomes is a very important step in the formation of haemosiderin from ferritin. The divested iron cores of these 'siderosomal ferritins' are unstable and could easily be transformed into finer particles, typical of haemosiderin. However, a third view maintains that it has still not been definitively established that all haemosiderin really is a product of ferritin [16,21]. Other possible sources for haemosiderin iron are senescent or defective developing erythrocytes.

Hereditary haemochromatosis

In some cases the body's iron balance is disturbed. If, over a prolonged period, less iron is absorbed than lost, iron deficiency will develop. In contrast, if more iron is absorbed than lost, iron will accumulate in the liver and in other tissues. This is the case in

hereditary haemochromatosis. Hereditary haemochromatosis - also called idiopathic or primary haemochromatosis - is an autosomal recessive genetic disorder characterized by excessive gastrointestinal iron absorption and progressive iron loading of parenchymal cells [22-24]. After some time, at about the age of forty, most homozygotes will present one or more of the following symptoms: hepatic fibrosis, cirrhosis, skin pigmentation, endocrine abnormalities and cardiomyopathy. Ferritin and haemosiderin concentrations and transferrin saturation are always increased, while serum ferritin concentrations are often elevated [25-27]. Regular phlebotomy can prevent organ damage, provided that the disorder is recognized early in life, which is usually not the case [26,27].
It is estimated that about 0.3% of the population may be homozygote for the gene and 10% may be heterozygote. The heterozygotes are usually not ill [27]. Recently, it has been increasingly suggested that what is now a "disease gene" may initially have been a "nutritional supplement gene" [23,28], when iron supplementation and improved nutrition were not the norms.

Secondary haemochromatosis

Secondary haemochromatosis is iron overload caused by certain other diseases or by their treatment. Usually, there is an ineffective erythropoiesis leading to anaemia without an iron deficiency [29]. The body tries to compensate for the ineffective erythropoiesis by increasing the production of red blood cells. This is accompanied by an increased gastrointestinal absorption of iron for haem synthesis. At the same time blood transfusions may be necessary to suppress the anaemia. These blood transfusions and the increased uptake of iron will lead to iron overload at an early age [30].

Harmful effects of iron

As long as iron is in ferritin and in the oxidized state, it is soluble and non-toxic. *In vivo*

and *in vitro*, ferritin and haemosiderin iron can be mobilized by reducing agents such as NADH and O_2^- [31,32]. Mobilized iron may get involved in radical reactions [33-35], such as the Haber-Weiss reaction (Figure 1.4). The hydroxyl radical (OH·) produced in these reactions is extremely harmful to DNA, proteins and lipids in membranes [36].

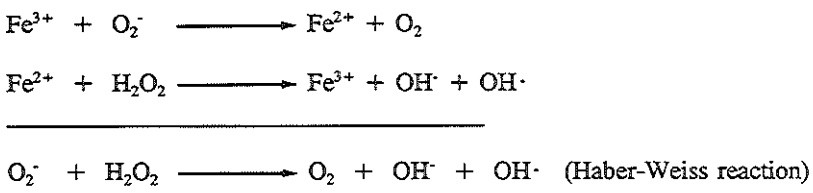

Figure 1.4
Iron catalyses the Haber-Weiss reaction, in which the harmful hydroxyl radical is formed.

REFERENCES

1. **Rossander L, Hallberg L, Björn-Rasmussen E** (1979) Absorption of iron from breakfast meals. Am J Clin Nutr 32:2484-2489
2. **de Jong G, van Dijk JP, van Eijk HG** (1990) The biology of transferrins - Critical review. Clin Chim Acta 190:1-46
3. **Theil EC** (1987) Ferritin: structure, gene regulation and cellular functions in animals, plants and microorganisms. Annu Rev Biochem 56:289-315
4. **Drysdale JW** (1977) Ferritin phenotypes: structure and metabolism. Jacobs A (ed) In: Iron metabolism. Elsevier, Amsterdam, pp. 41-57
5. **Rouault TA, Hentze MW, Caughman SW, Harford JB, Klausner RD** (1990) Binding of a cytosolic protein to the iron-responsive element of human ferritin messenger RNA. Science 241:1207-1210
6. **Leibold EA, Munro HN** (1988) Cytoplasmic protein binds in vitro to a highly conserved

sequence in the 5' UTR of ferritin heavy- and light-subunit mRNAs. Proc Natl Acad Sci USA 85:2171-2175

7. **Levi S, Luzzago A, Cesareni G, Cozzi A, Franceshinelli F, Albertini A, Arioso P** (1988) Mechanism of ferritin iron uptake: activity of the H-chain and deletion mapping of the ferro-oxidase site. J Biol Chem 263:18086-18092
8. **Lawson DM, Treffry A, Artymiuk PJ, Harrison PM, Yewdale SJ, Luzzago A, Cesarani G, Levi S, Arioso P** (1989) Identification of the ferroxidase centre in ferritin. Febs Lett 254:207-210
9. **Michaelis L, Coryell CD, Granick S** (1943) Ferritin: III The magnetic properties of ferritin and some other colloidal ferric compounds. J Biol Chem 148:463-480
10. **Myagkaya GC, de Bruijn WC** (1982) X-ray microanalysis of cellular localization of ferritin in mammalian spleen and liver. Micron 13:7-21
11. **Treffry A, Harrison PM, Cleton MI, de Bruijn WC, Mann S** (1987) A note on the composition and properties of ferritin iron-cores. J Inorg Biochem 31:1-6
12. **Treffry A, Lee PJ, Harrison PM** (1984) Iron-induced changes in rat liver isoferritins. Biochem J 220:717-722
13. **Mattia E, den Blaauwen J, van Renswoude J** (1990) Role of protein synthesis in the accumulation of ferritin mRNA during exposure of cells to iron. Biochem J 267:553-555
14. **Worwood M** (1979) Serum ferritin. CRC Crit Rev Clin Lab Sci 10:171-204
15. **Wixom RL, Prutkin L, Munro HN** (1980) Hemosiderin: nature, formation and significance. Int Rev Exp Pathol 22:193-224
16. **Fischbach FA, Gregory DW, Harrison PM, Hoy TG, Williams JM** (1971) On the structure of hemosiderin and its relationship to ferritin. J Ultrastruct Res 37:495-503
17. **Bell SH, Weir MP, Dickson DPE, Gibson JF, Sharp GA, Peters TJ** (1984) Mössbauer spectroscopic studies of human haemosiderin and ferritin. Biochim Biophys Acta 787:227-236
18. **Andrews SC, Brady MC, Treffry A, Williams JM, Mann S, Cleton MI, de Bruijn WC, Harrison PM** (1988) Studies on haemosiderin and ferritin from iron-loaded rat liver. Biol Metals 1:33-42
19. **Hoy TG, Jacobs A** (1981) Ferritin polymers and the formation of haemosiderin. Br J Haematol 49:593-602
20. **Richter GW** (1983) Cellular ferritin overload and formation of hemosiderin. In:

Urishizaki I, Aisen Ph, Listowsky I, Drysdale JW (eds) Structure and function of iron storage and transport proteins I. Elsevier, Amsterdam, pp.155-162

21. **St. Pierre TG, Pollard RK, Dickson DPE, Ward RJ, Peters TJ** (1988) Mössbauer spectroscopic studies of deproteinised, sub-fractionated and reconstituted ferritins: the relationship between haemosiderin and ferritin. Biochim Biophys Acta 952:158-163
22. **Simon M, Bourel M, Genetet B, Fauchet R** (1977) Idiopathic hemochromatosis. Demonstration of recessive inheritance and early detection by family HLA typing. N Eng J Med 297:1017-1021
23. **Edwards CQ, Skolnick MH, Kushner JP** (1981) Hereditary hemochromatosis: contributions of genetic analyses. Prog Hematol 12:43-71
24. **van Deursen** (1989) Iron content of liver tissue. A biochemical, histological and clinical study, especially in hereditary haemochromatosis. PhD Thesis, University of Limburg, the Netherlands
25. **van Suylen JDE, Leijnse B** (1989) Serumferritine. Tijdschrift NVKC 14:12-18
26. **Niederau C, Fisher R, Sonnenberg A, Stremmel W, Trampisch HJ, Strohmeyer G** (1985) Survival and cause of death in cirrhotic and noncirrhotic patients with primary hemochromatosis. N Engl J Med 313:1256-1262
27. **Edwards CQ, Griffen LM, Goldgar D, Drummond C, Skolnick MH, Kushner JP** (1988) Prevalence of hemochromatosis among 11,065 presumably healthy blood donors. N Engl J Med 318:1355-1362
28. **Johnson RB** (1988) Advantageous hemochromatosis. N Engl J Med 319:1155-1156
29. **Bottomley SS** (1980) Sideroblastic anaemia. In: Jacobs A, Worwood M (eds) Iron in biochemistry and medicine II. Academic Press, London, pp. 363-392
30. **Bridges K** (1988) Transfusion hemosiderosis. In: Transfusion medicine. Churchill WH, Kurtz SR (eds) Blackwell Scientific Publications, Oxford, pp. 129-144
31. **O'Connell MJ, Peters TJ** (1987) Ferritin and haemosiderin in free radical generation, lipid peroxidation and protein damage. Chem Phys Lipids 45:241-249
32. **Topham R, Goger M, Pearce K, Schultz P** (1989) The mobilization of ferritin iron by liver cytosol. A comparison of xanthine and NADH as reducing substrates. Biochem J 261:137-143
33. **Halliwell B, Gutteridge JMC** (1986) Iron and free radical reactions: two aspects of antioxidant protection. Trends Biochem Sci 11: 372-375

34. **Bacon BR, Britton RS** (1990) The pathology of hepatic iron overload. A free radical-mediated process? Hepatology 11:127-137

35. **Biemond P, Swaak AJG, van Eijk HG, Koster JF** (1988) Superoxide dependent iron release from ferritin in inflammatory diseases. Free Rad Biol Med 4:185-198

36. **Wolff SP, Garner A, Dean RT** (1986) Free radicals, lipids and protein degradation. Trends Biochem Sci 11:27-31

CHAPTER 2

MATERIALS & METHODS

(GENERAL)

CHEMICALS

All chemicals used were of analytical grade.

A. BIOCHEMICAL METHODS

Animals

Male Wistar rats (TNO, Zeist, The Netherlands) were 3 months old at the beginning of the experiments.

Parenteral iron-loading

Rats were given four intraperitoneal injections of iron dextran (50 mg/ml Imferon, Fisons, U.K.) in a total dose of 100 mg Fe(III) spread over a period of 4 weeks. After the last injection of Imferon the rats received no further treatment for a period of 4 weeks (resting period). Immediately after the resting period the livers were processed.

Dietary iron-loading

Rats were fed on standard pellet food enriched with 2% (w/w) carbonyl iron (Sigma) for a period of 5 months and their livers were subsequently processed.

Perfusion of the rat liver

Rats were anaesthetized intraperitoneally using 0.7 ml pentobarbital (Academic Hospital Dijkzigt, Rotterdam). The blood from the liver was washed out by a brief perfusion through the portal vein with 0.15 M NaCl, flow 20-25 ml/min. The liver was removed, weighed, a small piece of liver was dried for the determination of non-haem liver iron content and the rest of the liver was frozen in liquid nitrogen and stored at -20°C until they were fractionated.

Fractionation of the liver

Fractionation was performed as described by Richter [1]. To summarize, the homogenate, prepared in 0.3 M sucrose, was centrifuged twice yielding a supernatant, i.e. the (ferritin-containing) cytosolic fraction, and a pellet. This pellet was layered on a discontinuous sucrose gradient (1.4-2.2 M) yielding a pellet (the heavy lysosomes = siderosomes) and several bands, including the lighter lysosomes. Arylsulphatase A (EC 3.1.6.1) activity of lysosomes [2] was detected using the *arylsulphatase assay*: 0.2 ml sample was mixed with 0.2 ml substrate buffer (0.02 M *p*-nitrocatechol sulphate (= 2-hydroxy-5-nitrophenylsulphate), dipotassium salt (Sigma) in 0.5 M sodium acetate buffer, pH 5.5) and incubated at 37°C. After 15 min the reaction was stopped by adding 1 ml 1 M NaOH. Release of 4-nitrocatechol was measured spectrophotometrically at 515 nm. The molecular extinction coefficient of 4-nitrocatechol: 11,200 liter M^{-1} cm^{-1} was used to calculate activities.

Preparation of haemosiderin

Haemosiderin was prepared as described by Vidnes and Helgeland [3]. The lysosomal fraction was subjected to osmotic shock with bidistilled water, sonicated for 1 min with a vibra cell, position 5, and centrifuged for 10 min at 10,000 *g*, 4°C in a Beckman centrifuge type J-21c, rotor Ja-20. The resulting supernatant was used for the preparation of lysosomal ferritin (see "preparation of ferritins"). The pellet was resuspended in 6 vol 0.15 M NaCl and centrifuged for 10 min at 10,000 *g*, 4°C. This action was repeated once. The resulting pellet was resuspended in 2 vol bidistilled water and sonicated for 1 min, position 5. This suspension was centrifuged for 10 min at 25,000 *g* and the pellet was resuspended in bidistilled water. This was repeated twice. Next, the pellet was frozen in liquid nitrogen and thawed with bidistilled water to remove a grey-brown layer. The suspension was centrifuged for 10 min at 5000 *g*, 4°C. The pellet was resuspended in as little bidistilled water as possible and stirred for 24 h at 4°C. Finally, the suspension was centrifuged for 10 min at 3000 *g*, 4°C. The resulting pellet, representing haemosiderin was resuspended in bidistilled water or in 0.15 M NaCl. Half of the haemosiderin was further purified by centrifugation through 4.1 M KI (Merck, Ref.4). After removing the

KI by washing with bidistilled water, the haemosiderin was lyophilized and solubilized in 20 mM tetramethylammonium hydroxide pentahydrate (Aldrich Chemie).

Preparation of ferritins

The cytosolic fraction and the supernatant of the sonicated lysosomes (see "preparation of haemosiderin") were treated in the same way for the isolation of ferritin [5].
After heating for 10 min at 80°C and cooling on ice, both suspensions were centrifuged twice for 45 min at 3000 *g*, 4°C in a Beckman centrifuge type J-21c, rotor Ja-20. Supernatants were centrifuged in a Beckman ultracentrifuge type L5-65, rotor Ti-60 for 60 min at 78,000 *g*, 4°C. Pellets were collected, suspended in 0.15 M NaCl and subjected to 7000 *g* for 60 min in the Ja-20 rotor. The resulting supernatants were centrifuged twice in the Ti-60 rotor for 60 min at 95,000 *g*, 4°C and the pellets containing the ferritins were suspended in 0.15 M NaCl.

Gel electrophoresis and Western blotting

Non-denaturing polyacrylamide gel electrophoresis (PAGE) was carried out in 5% gels using Tris-glycine (pH 8.3) or in Pharmacia precast PAA 2/16 or PAA 4/30 gels following manufacturer's instructions, in a Pharmacia GE 2/4 chamber. Gels were stained for protein with Coomassie brilliant blue G-250 (Serva) and for iron with 2% $K_4Fe(CN)_6$ in 2% HCl. Samples and markers (Pharmacia HMW and LMW kit) were dissociated into subunits by heating (100°C, 5-10 min) in the presence of 2% (w/v) sodium lauryl sulphate (SDS) and 20 mM dithiothreitol just before electrophoresis. SDS-PAGE was carried out in 15% polyacrylamide gels using the Laemmli buffer system [6] or in Pharmacia precast gradient gels. Gels were stained for protein with Coomassie brilliant blue G-250. For blotting SDS-PAGE was carried out in 18% gels in a Bio-Rad Mini Protean II cell followed by electrophoretic transfer blotting in a Bio-Rad Mini Trans Blot cell. Nitrocellulose membranes were either stained using Amido black or blocked with gelatin and subsequently incubated with rabbit anti-(rat liver ferritin) serum [7] overnight. This was followed by washing and incubation with alkaline-phosphatase-conjugated goat anti-rabbit IgG (Bio-Rad). Immunostaining was performed according to manufacturer's

instructions.

Amino acid analysis

Hydrolysis:

Approximately 25 μl ferritin (1 mg/ml) was mixed with 15 μl internal standard (Nleu, Sigma), 150 μl 4 M *p*TSA (Pierce, U.S.A.) and 10 μl 2% 3-(2 aminoethyl)indol. Hydrolysis was carried out in vacuo <1 mmHg, at 110°C, for a period of 24 h. The hydrolysate was neutralized with 1 M NaOH until it reached pH 2.0. To prevent toxication of the amino acid separation resin with the considerable amount of Fe^{3+}, 0.1% EDTA disodium was added to the hydrolysate (end concentration 0.01%).

Analysis:

An aliquot of 50 μl was analysed, using a lithium citrate program with orthophtalaldehyde as reagent at a 4151 Alpha Plus (Pharmacia-LKB) according to the current manual. Using a D-2000 Chromato-Integrator (Merck-Hitachi) the mol% of all preparations was calculated, based on reference values of a commercial calibration mixture (Pierce, U.S.A.) [8].

To estimate *relatedness of proteins*, Marchalonis and Weltman [9] have defined the parameter $S\Delta Q$ (sum of the squared differences):

$$S\Delta Q = \sum_{1}^{j} (X_{i,A} - X_{i,B})^2$$

(A) and (B): the proteins which are to be compared;

X_i: the content of a given amino acid i;

j: the total number of amino acids.

For identical proteins $S\Delta Q$ is (close to) zero, as there are no differences. The greater the number of differences between two proteins, the higher the $S\Delta Q$ value.

Determination of iron and protein

Ferritin iron was determined as described by Harris [10] using ferrozine (Sigma). Absorbance was measured at 562 nm. Non-haem liver iron was determined at 530 nm as

described by Bobeck-Rutsaert [11] after destruction of approximately 10 mg (dry weight) liver with 1 ml concentrated $HClO_4$ and using ammonium iron(II) sulphate hexahydrate (Merck) as a standard. Protein was determined as described by Bradford et al. [12] and absorbance measured at 595 nm using bovine serum albumin (BSA) as a standard.

Immunoreactivity

Isolates were reacted with rabbit anti-(rat liver ferritin) antiserum [7] in an Ouchterlony immunodiffusion assay.

Isoelectric focusing (IEF)

Analytical IEF was conducted on thin (0.5 mm) slabs of agarose (Isogel Agarose-EF, Pharmacia LKB) containing Ampholines (pH 3.5-10 and pH 4-6, Pharmacia LKB) on Gel Fix for Agarose (Serva) following manufacturer's instructions (Pharmacia LKB note 1818 A). Slabs were cut to 4×5 cm to be used in PhastSystem (Pharmacia). Focusing conditions on agarose gels:

Sample applicator down at	1.2	0 Vh
Sample applicator up at	1.3	0 Vh

Sep 1.1	1000 V	2.5 mA	3.5 W	15°C	60 Vh
Sep 1.2	200 V	2.5 mA	3.5 W	15°C	15 Vh
Sep 1.3	1000 V	2.5 mA	3.5 W	15°C	205 Vh

Gels were stained using Coomassie brilliant blue R-250 (Merck) following manufacturer's instructions (Pharmacia LKB note 1818 A).

Preparative IEF was carried out as described for analytical IEF. Afterwards, gel slices containing the desired proteins were excised and placed in a tube containing 0.5 ml bidistilled water. After at least 48 h at 4°C, the water phase, containing the proteins from

the slices, was concentrated and stored at 4°C. The rest of the agarose gel was stained using Coomassie brilliant blue R-250.

Titration curve analysis

Titration curve analysis was used to analyse protein charge characteristics. It was conducted on agarose slabs prepared as described for IEF. In the first dimension a pH gradient was generated as described for analytical focusing. Electrophoresis in the second dimension:

Sample applicator down at		5.3	0 Vh
Sample applicator up at		5.3	6 Vh

Sep 5.1	1000 V	2.0 mA	3.5 W	15°C	150 Vh
Sep 5.2	0 V	0.0 mA	0.0 W	0°C	0 Vh
Sep 5.3	1000 V	2.0 mA	0.2 W	15°C	45 Vh

Isolation of hepatocytes [13]

Rats were anaesthetized intraperitoneally using 0.7 ml pentobarbital (Academic Hospital Dijkzigt, Rotterdam). After cannulation of the portal vein, perfusion was started with buffer containing 10 mM Hepes, 140 mM NaCl, 7 mM KCl, pH 7.6, 37°C, 12 ml/min. The flow rate was increased to 48 ml/min and perfusion was continued with buffer containing 100 mM Hepes, 66 mM NaCl, 7 mM KCl, 3.6 mM $CaCl_2 \cdot 2H_2O$, 1% (w/v) BSA and 0.05% (w/v) collagenase (type I, Sigma), pH 7.4. The final washing buffer contained 50 mM Hepes, 110 mM NaCl, 5 mM KCl, 0.74 mM $MgCl_2 \cdot 6H_2O$, 1.26 mM $CaCl_2 \cdot 2H_2O$ and 1% (w/v) BSA (pH 7.4) and was circulated. All buffers used were oxygenated (95% O_2/5% CO_2). The softened liver was excised and cells were loosened in 25 ml of the washing buffer. After filtration through two layers of wide maze gauze, hepatocytes in the filtrate were spun down for 30 sec at 50 *g*, 4°C. Cells were washed in the same buffer, frozen in liquid nitrogen in the presence of 4% (v/v) DMSO (Sigma) and stored at -20°C.

Fractionation of hepatocytes

Cells were rapidly thawed and the medium was replaced by fresh medium to remove DMSO (1 min, 200 *g*). Cells were fractionated as described for the whole liver (see "fractionation of the liver"), with the modification that throughout the procedure a tight pestle was used.

Isolation of nonparenchymal cells [14]

Rats were anaesthetized intraperitoneally using 0.7 ml pentobarbital (Academic Hospital Dijkzigt, Rotterdam). After cannulation of the portal vein, perfusion was started with Earl's buffered salt solution (EBSS, Gibco), pH 7.4, 37°C, 4 min at flow rate 10 ml/min. Perfusion was continued with EBSS containing 0.2% (w/v) Pronase E (Merck). All buffers used were oxygenated. The liver was excised, rinsed in ice-cold EBSS and cut into pieces. Under continuously shaking, the liver was incubated in 100 ml EBSS containing 0.2% Pronase E, pH 7.4, 37°C, for 60 min. The suspension was then filtered through nylon gauze (Kabel, Zaandam, The Netherlands) and the filtrate was spun for 5 min at 400 *g*. The supernatant was discarded and the pellet was resuspended in cold EBSS and was washed twice at 400 *g* for 5 min. The final pellet was suspended in EBSS (end volume 5 ml). This was mixed with 7 ml 30% (w/v) metrizamide (Nycomed, Norway) and an aliquot DNase I grade II (Boehringer). Thirty per cent metrizamide (pH 7.4) was prepared in EBSS without NaCl. If necessary, osmolarity was adjusted using NaCl. This mixture was divided between two tubes and on top 1 ml EBSS was layered. It was spun for 15 min at 1500 *g*. The brown cells were collected from the pellet. The pellet was washed by spinning for 10 min at 400 *g*. Finally, cells were frozen in liquid nitrogen after addition of 4% (v/v) DMSO (Sigma) and stored at -20°C.

Fractionation of nonparenchymal cells

After thawing the cells at 37°C, DMSO was replaced by EBSS (pH 7.4). Cells were incubated with 0.1 vol stock solution digitonin (Fluka) for 20 min at 0°C. Cells were resedimented (10 min in an Eppendorf centrifuge) and supernatants were used in enzyme assays.

Acid phosphatase assay: 100 mg citric acid and 232 mg trisodium citrate·$2H_2O$ were dissolved in 25 ml bidistilled water (pH 4.8). Then, 51 mg 4-nitrophenylphosphate was added. This mixture was stored at 4°C (not longer than 7 days). One ml of this mixture was incubated with 50 μl supernatant and 0.2 ml water for 30 min at 30°C. The reaction was stopped using 2.0 ml 0.1 M NaOH. Absorbance was measured at 405 nm.
Lactate dehydrogenase assay: 0.1 ml supernatant was mixed with 2 ml substrate buffer (0.93 mM sodium pyruvate (Boehringer) in 0.05 M phosphate buffer, pH 7.5) and 1 ml 0.56 mM NADH. The decrease in absorbance at 340 nm was monitored for 3 min.
For both assays "total latency" was based on results in the presence of 1% (v/v) Triton X-100.

B. ANALYTICAL ELECTRON MICROSCOPY

In order to enhance the readability of this thesis, the following pages provide a short overview of the principles of the electron microscopic techniques that were used.
In conventional transmission electron microscopy (CTEM), images are generated by a high-energy (80 kV) electron beam (primary beam, $E=E_0$) passing through an ultrathin-sectioned specimen. Incident electrons can either pass the specimen unscattered ($E=E_0$), or be scattered due to interaction with atoms in the specimen (Figure 2.1) [15].
Interaction with shell electrons in the specimen results in inelastic scattering. Inelastically scattered electrons are scattered over low angles with respect to the direction of the primary electron beam and, in addition, have lost a variable amount of energy ($E=E_0-\Delta E_i$; i variable). Since they are polyenergetic/polychromatic and hence focused at different image planes, contrast and resolution in the final image deteriorate. However, for analytical purposes element-specific energy loss can be used in electron spectroscopy (for details see: electron spectroscopy, pp. 23-26).
Interaction with atomic nuclei in the specimen results in elastic scattering, which is characterized by a small loss in energy ($E\approx E_0$) and large angle scattering (0-180°). High-angle scattered electrons are excluded from image formation by the objective lens

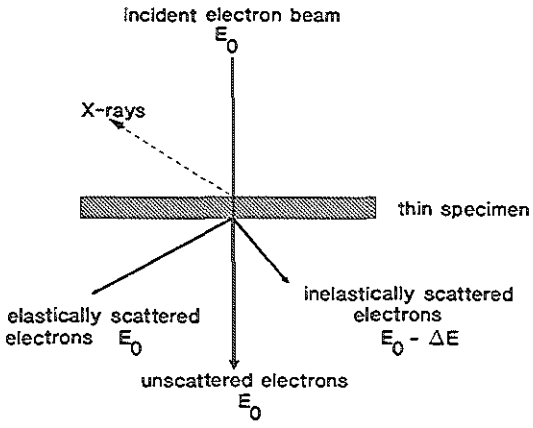

Figure 2.1

Interactions of an electron beam with a thin specimen

diaphragm. By this exclusion, image contrast is produced, so the higher the incidence of elastic scattering under large angles, the more enhanced the contrast is. Since elastic scattering is proportional to the atomic mass (*Z* number), heavy metal ions, such as lead and uranium, are used to stain specimens for contrast enhancement in CTEM.
Special effects of inelastic scattering are excitation and ionization. In both cases shell electrons are removed from their energy level by incident beam electrons and electron vacancies are created. When an electron from an outer shell fills a vacancy, shell/element specific X-ray photons representing the difference in shell energy between the outer shell and the shell with the vacancy, are emitted. Aspecific X-rays are generated through retardation of beam electrons passing in the vicinity of atomic nuclei in the specimen. These aspecifically generated X-rays are called Bremsstrahlung or continuum X-rays. Their energy band ranges from 0 to approximately 76 kV if 80 kV electrons are used in

the primary beam. The amount of X-rays is related to the total mass irradiated by the primary beam [16]. Both specific and aspecific X-rays are used for analytical purposes (for details see: electron probe microanalysis, pp. 27-28).

In this study two types of analytical transmission electron microscopes were used [17]:

(1) a Zeiss EM 902 with an in-column electron spectrometer. Electron spectroscopic images (*ESI*) and spectra (*EELS*) can be obtained.

(2) a Philips EM 400 with a LaB_6 cathode and a Tracor Northern TN2000 X-ray microanalyser for electron probe microanalysis (*EPMA*).

Electron spectroscopy

The Zeiss EM 902 is equipped with a spectrometer of the prism-mirror-prism type according to Castaign/Henry/Ottensmeyer [18], integrated in column. Using this spectrometer electrons can be separated according to their energy in an energy loss spectrum (Figure 2.2) by moving a pre-chosen interval of ΔE over the energy selecting slit of the spectrometer. Electron energy-loss spectra (beam intensity records (I%) versus energy loss (ΔE)) are acquired by a photomultiplier (PMT) and are recorded directly on a plotter.

For image formation, besides the objective lens excluding large angle scattered electrons, the energy selecting slit is introduced as a second selection mechanism [19,20]. The width of the spectrometer slit determines the size of the interval of imaging electrons, making the image virtually monoenergetic/monochromatic. The position of the slit in the energy band can be chosen. In theory, if a high-contrast image of unstained material (Figure 2.2 and 2.3A) is desired, the slit is positioned around $\Delta E=0$, producing a monoenergetic zero-loss image. If an element-specific image is desired, for instance an Fe-specific image, the slit is positioned around the ionization edge (just before the peak) of iron ($\Delta E=708$ eV). However, such images still contain electrons with aspecific energy losses.

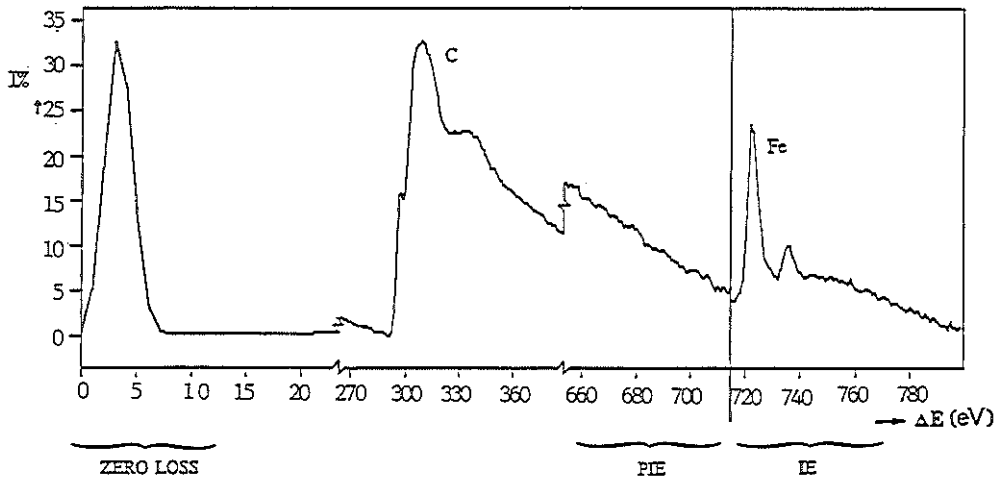

Figure 2.2

Composed example of an electron energy loss spectrum, showing the positions of the energy selecting slit to produce a zero loss, a PIE and an IE image.

To separate the two populations within the slit width two images are made: one below the edge, called PIE (pre-ionization edge) image (Figure 2.2 and 2.3B) and one beyond the edge, called the IE (ionization edge) image (Figure 2.2 and 2.3C). Subtraction of the PIE image from the IE image results in a (semi-)net-intensity element distribution image. This subtraction can be performed photographically or by computer-assisted image processing, e.g. using the IBAS image analyser [21].

In practice, the slit of the spectrometer is not moved, but maintained in the optical axis of the microscope, thus allowing only electrons with $E=E_0$ to pass through (Figure 2.4A). In this manner a zero-loss image is obtained. The element-related PIE and IE images are obtained by increasing the energy of the primary beam by ΔE to $E_0+\Delta E$. As the slit of the spectrometer is maintained in the optical axis, all electrons with energy loss ΔE will

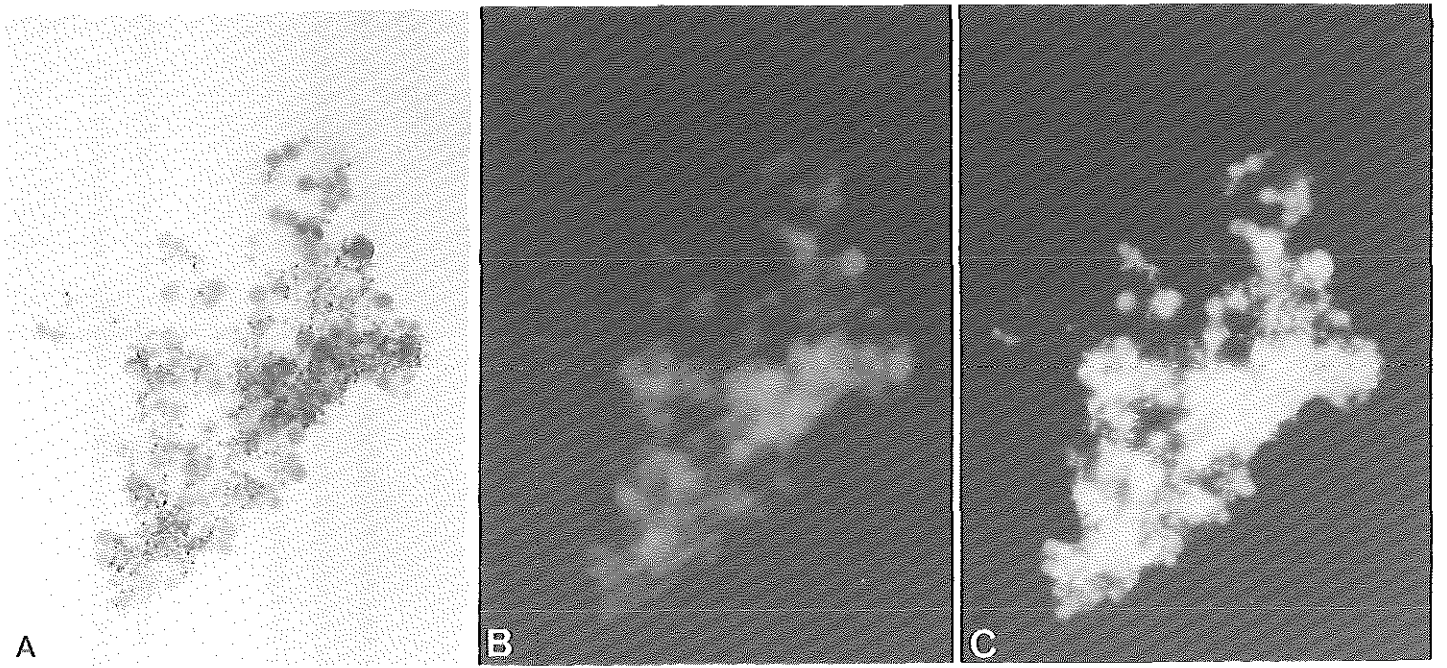

Figure 2.3

(A) Zero-loss image taken around ΔE=0 eV. (B) PIE image taken around ΔE=680 eV. (C) IE image taken around ΔE=720 eV. Subtraction of B from C would yield an Fe-specific image.

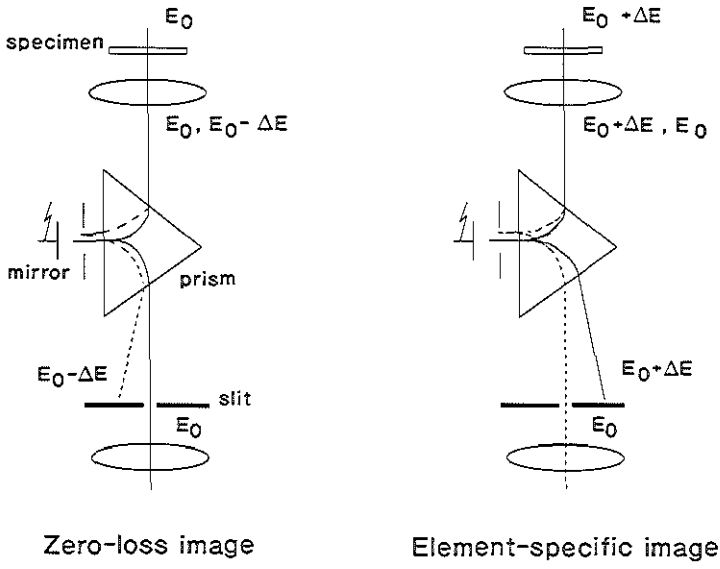

Figure 2.4

(A) To obtain a zero-loss image, the slit is positioned so that solely unscattered and under a small angle elastically scattered, monoenergetic electrons, with an energy loss $\Delta E=0$ eV can pass through it. (B) To obtain an Fe-specific image, the slit is kept in the same position as under A, whereas the energy of the primary beam is increased by 708 eV (ΔE_{Fe}). As a consequence, only electrons with an energy loss of around 708 eV can pass the slit.

be able to pass the slit, whereas other electrons are blocked (Figure 2.4B). The passage of electrons through the slit will yield an increase in intensity over a continuum of aspecific energy losses (background) (Figure 2.2 and 2.3).

Image analysis

Microscopic images of samples are recorded by video camera and transferred to the image analyser IBAS 2000 for determination of mean iron-core diameters [21].

Electron probe microanalysis

This technique uses, in a conventional transmision electron microscope, the shell/element specific X-ray photons (peaks) and the continuum X-rays (background). X-rays are registered by a SiLi detector connected to a multichannel analyser in the X-ray microanalyser (Tracor Northern, TN2000). The amount of X-rays is proportional to the number of atoms irradiated by electrons in the beam, within a constant dwell time per point. In order to acquire X-rays a focused spot of electrons, with a constant diameter, is moved within a small area of the sample material. Registered X-rays, quantified as counts, are arranged in channels according to their energy, forming a spectrum of specific peaks over a continuum (background of aspecific X-rays) (Figure 2.5). Peaks are identified by their position on the energy scale. In practice, the peaks are identified automatically by an available peak identification program [22].

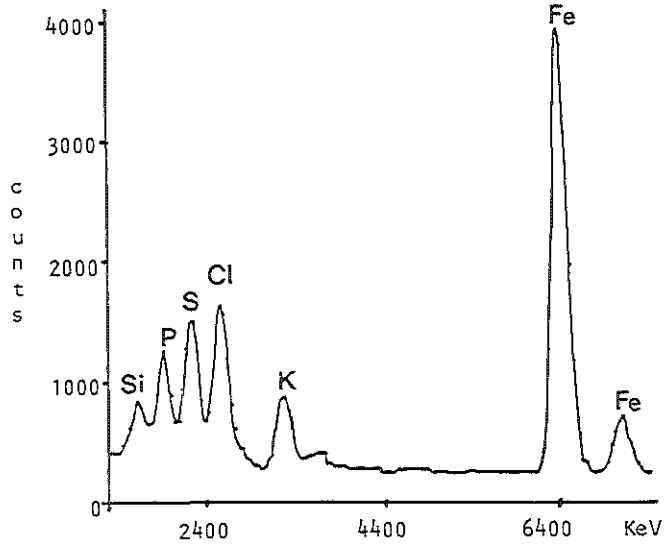

Figure 2.5

EPMA energy spectrum. Peaks are identified by the peak identification program of the microanalyser.

Net-intensity values (i.e. peak-background) are obtained by the introduction of regions of interest (ROI; 6240-6520 KeV for Fe and 1880-2160 KeV for P was used) around the identified peaks and calculation by the energy filter program of the TN2000 computer software. In these ROI a computer program calculates the local continuum contribution, which is subtracted from the total contents of the ROI, leaving the element-related net-intensity values. Subsequently, iron/phosphorus mass ratios, which are generated simultaneously in one spot, are calculated from net-intensity values by the peak ratio program.

REFERENCES

1. **Richter GW** (1984) Studies of iron overload. Rat liver siderosome ferritin. Lab Invest 50:26-35
2. **Baum H, Dodgson KS, Spencer B** (1959) The assay of arylsulphatases A and B in human urine. Clin Chim Acta 4:453-455
3. **Vidnes A, Helgeland L** (1973) Sex and age differences in the hemosiderin content of rat liver. Biochim Biophys Acta 328:365-372
4. **McKay RH, Fineberg RA** (1964) Horse spleen haemosiderin I. Isolation. Arch Biochem Biophys 104:487-495
5. **Penders TJ, de Rooij-Dijk HH, Leijnse B** (1968) Rapid isolation of ferritin by means of ultracentrifugation. Biochim Biophys Acta 168:588-590
6. **Laemmli UK** (1970) Cleavage of structural proteins during the assembly of the head of bacteriophage T4. Nature 227:680-685
7. **Mostert LJ, Cleton MI, de Bruijn WC, Koster JF, van Eijk HG** (1989) Studies on ferritin in rat liver and spleen during repeated phlebotomy. Int J Biochem 21:39-47
8. **van Eijk HG, van Noort WL** (1986) The liability of the use of *p*-toluenesulfonic acid for simultaneous hydrolysis and quantitation of both *N*-acetyl glucosamine and amino acids in human transferrins. Clin Chim Acta 157:305-310
9. **Marchalonis JJ, Weltman JK** (1971) Relatedness among proteins: a new method of estimation and its application to immunoglobulins. Comp Biochem Physiol 38B:609-625
10. **Harris DC** (1978) Iron exchange between ferritin and transferrin in vitro. Biochemistry

17:3071-3078

11. **Bobeck-Rutsaert MMJC** (1974) PhD Thesis, University of Rotterdam, The Netherlands
12. **Bradford MM** (1976) A rapid and sensitive method for the quantification of microgram quantities of proteins utilizing the principles of protein-dye binding. Anal Biochem 72:248-251
13. **Dekker CJ, Kroos MJ, van der Heul C, van Eijk HG** (1985) Uptake of sialo and asialo transferrins by isolated rat hepatocytes. Comparison of a heterologous and a homologous system. Int J Biochem 17:701-706
14. **Knook DL, Blansjaar N, Sleyster EC** (1977) Isolation and characterization of Kupffer and endothelial cells from the rat liver. Exp Cell Res 109:317-329
15. **Misell DL** (1978) Image analysis, enhancement and interpretation. In: Glauert A (ed) Practical methods in electron microscopy. North Holland Publishing Company, Amsterdam, pp. 21-31
16. **Chandler JA** (1977) X-ray microanalysis in the electron microscope. In: Glauert A (ed) Practical methods in electron microscopy, volume 5, part II. North-Holland Publishing Company, Amsterdam, pp. 317-547
17. **Cleton-Soeteman MI, de Bruijn WC, van Eijk HG** (1989) Nieuwe ontwikkelingen in de detectie en chemische microanalyse van ijzer. Tijdschrift NVKC 14:205-213
18. **Ottensmeyer FP, Andrew JW** (1980) High-resolution microanalysis of biological specimens by electron energy loss spectroscopy and by electron spectroscopic imaging. J Ultrastruct Res 72:336-348
19. **Reimer L, Fromm I, Rennekamp R** (1988) Operation modes of electron spectroscopic imaging and electron energy-loss spectroscopy in a transmission electron microscope. Ultramicroscopy 24:339-354
20. **Egerton, RF (1986)** Electron energy-loss spectroscopy in the electron microscope. Plenum Press, New York
21. **Sorber CJW, van Dort JB, Ringeling PL, Cleton-Soeteman MI, de Bruijn WC** (1990) Quantitative energy-filtered image analysis in cytochemistry II. Morphometric analysis of element-distribution images. Ultramicroscopy 32:69-78
22. **de Bruijn WC, van Miert MPC** (1988) Extraneous background-correction program for matrix bound multiple point X-ray microanalysis. Scan Micros 2:319-322

CHAPTER 3

CYTOSOLIC AND SIDEROSOMAL FERRITINS

The effect of dialysis on iron to phosphorus ratios

SUMMARY

Cytosolic and siderosomal ferritin, and haemosiderin were isolated from rat livers which had been iron-loaded by four intraperitoneal injections of iron-dextran. The cytosolic and siderosomal ferritins, prepared in a phosphate-free medium, were subjected to gel filtration chromatography on Sepharose 6B, yielding four fractions: a cytosolic monomeric (CMF) and void volume ferritin fraction (CVVF), and a siderosomal monomeric (SMF) and void volume ferritin fraction (SVVF). Of each fraction the iron to phosphorus (Fe/P) ratio and the effect of dialysis on this ratio was examined using electron probe microanalysis (EPMA). The Fe/P ratio of haemosiderin was determined before and after extensive purification. The following results were obtained: the Fe/P ratios as determined in CMF and in haemosiderin were not affected by dialysis or extensive purification, respectively. The Fe/P ratio in CVVF was affected by dialysis. In the siderosomal fractions only a trace of phosphorus (SVVF) or no phosphorus (SMF) was detected.

Our conclusion is that the phosphorus present in ferritin and haemosiderin is firmly bound; haemosiderin, if derived from ferritin, must have taken up phosphorus in the siderosomes.

The ferritin core contains, besides iron, also phosphorus, oxygen and hydrogen. The iron-core of ferritin from horse spleen can be represented by $(FeOOH)_8(FeO\text{-}OPO_3H_2)$ [1], with an atomic Fe/P ratio of about 9. However, several studies [2,3] have shown that this ratio varies among tissues and among species. It has been suggested [2] that the ratio is dependent on the iron content of the ferritin molecule. Subsequently, the question was raised as to whether phosphorus is an integral part of the iron core, or whether it is only loosely bound at surface positions of iron-core microcrystals.
From previous work [4], we know that the Fe/P ratios of siderosomal and cytosolic ferritins from iron-loaded rat livers, prepared in phosphate buffer, are influenced by dialysis. We now seek to establish the Fe/P ratios of the various ferritin fractions and haemosiderin, and the effect of dialysis (in the case of the ferritins) and further purification (in the case of the haemosiderin) on these ratios when phosphorus is excluded during the whole isolation procedure. In the work described in this chapter we have used a rat model, iron-loaded by intraperitoneal injections of iron-dextran. The Fe/P ratios are determined by electron probe micro analysis (EPMA).

RESULTS

Chromatography

The livers of 16 iron-loaded rats were pooled and used for the preparation of a cytosolic and a siderosomal (iron-rich lysosomes) fraction. After separation on Sepharose 6B the ferritin isolated from the cytosolic fraction yielded a main peak at the position of monomeric ferritin. Hence, we called this fraction cytosolic monomeric ferritin (CMF). A smaller peak eluted at the position of the void volume (called by us cytosolic void volume ferritin, CVVF). The position of the void volume was determined by Blue Dextran 2000. The ferritin isolated from the siderosomal fraction yielded a main peak at the position of the void volume fraction (called siderosomal void volume ferritin, SVVF) and a much smaller peak at the position of monomeric ferritin (called siderosomal mono ferritin, SMF) (Figure 3.1).

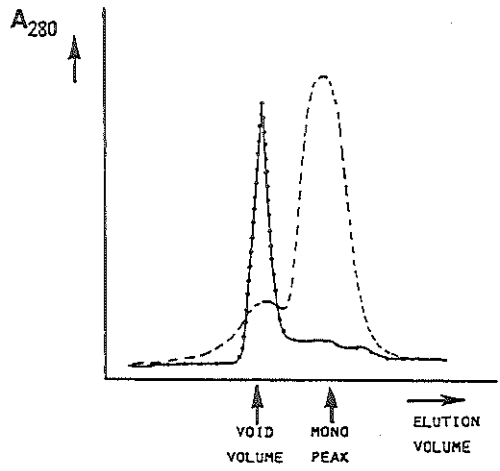

Figure 3.1
Chromatography of siderososomal (-o-o-) and cytosolic (—) ferritin on Sepharose 6B

Iron/phosphorus ratios

In order to study the presence of phosphorus and the effect of dialysis (ferritin samples) or of further purification (haemosiderin), Fe/P ratios before and after treatment were determined by EPMA. The EPMA results are summarized in Table 3.1.

Fe/P ratios were established in CMF, CVVF and in haemosiderin; The values were found to be different in each of the three fractions. In SMF no phosphorus was detected and in SVVF only a trace. Dialysis had no significant effect on the Fe/P ratio of CMF but a slight effect on that of CVVF; extensive purification with potassium iodide (KI) had no effect on the Fe/P ratio of haemosiderin.

DISCUSSION

To determine Fe/P ratios in cytosolic ferritin, siderosomal ferritin and haemosiderin we preferred to use EPMA [5] to the usual colorimetric techniques because the latter appeared to be insufficiently sensitive to detect very low amounts of phosphorus. In our material, which was not prepared in phosphate buffer, there is a marked difference in

Table 3.1

Fe/P ratios before and after dialysis as measured by EPMA

Fraction	Dialysis	Fe/P			
		mean ± SD	range	*n*	*t*-test
CMF	-	34.6 ± 10.5	22.1-56.7	20	
					n.s.
	+	33.0 ± 8.5	18.7-48.3	20	
CVVF	-	10.9 ± 3.7	5.9-15.9	20	
					$p<0.05$
	+	18.4 ± 4.2	13.5-25.5	20	
SMF	-	no P	-	20	
					n.d.
	+	-	-	20	
SVVF	-	no P/trace	-	20	
					n.d.
	+	no P/trace	-	20	
HS	-	16.1 ± 2.6	14.7-18.8	20	
					n.s.
HS	KI	16.9 ± 3.1	12.1-18.9	20	

Instrumental conditions: spot diameter:1μm; dwell time/determination:100 sec; tilt angle 18°; n.s.=not significant; *n*=number of determinations; n.d.=not determined;

the Fe/P ratios between cytosolic and siderosomal ferritins isolated from pooled iron-loaded rat livers. The siderosomal fractions contain only a trace of phosphorus (SVVF) or no phosphorus at all (SMF). In contrast, the cytosolic fractions CMF and CVVF and the haemosiderin do contain phosphorus. Assuming incorporation of cytosolic ferritin into the siderosomes, the results suggest that somehow during this process ferritin loses its phosphorus. When haemosiderin is formed, phosphorus is again attached to the ferric oxyhydroxide core. The mechanism, however, remains unclear. Although the presence of acid phosphatase activity is acknowledged in iron-containing lysosomes [6], a correlation between enzyme activity and the phenomenon as described here has not yet been demonstrated.

The Fe/P ratios found in this study for the major ferritin fractions, i.e. the CMF (34:1) and the SVVF (no phosphorus), are similar to the ratios described in previous studies [4] for unfractionated cytosolic (36:1) and siderosomal ferritin (no phosphorus) prepared in phosphate buffer and dialysed for 5 days. Apparently, this material had taken up phosphate during the isolation procedure, which is in line with in vitro experiments [7]. As the Fe/P ratios of the main cytosolic fraction CMF and the haemosiderin do not change significantly after extensive dialysis or further purification, respectively, we can conclude that the phosphorus in the ferritin and haemosiderin as prepared by our method is firmly bound. The change in the ratio in the CVVF, which is a fraction of all particles larger than 2000 kDa, may be due to phosphorus-containing compounds in which the phosphorus is affected by dialysis.

In summary, our experiments have shown that, in the cytosol of iron-loaded rat livers, mainly monomeric ferritin is present, which contains phosphorus. Once isolated under phosphate free conditions, the Fe/P ratio is not affected by dialysis. In the siderosomes of iron-loaded rat livers very little monomeric ferritin is present. This fraction contains only a trace of phosphorus. Neither of the siderosomal ferritin fractions contains phosphorus, in contrast to haemosiderin, in which the relative amount of phosphorus has doubled compared to cytosolic ferritin. Hence, any haemosiderin that was derived from ferritin must have taken up phosphorus in the siderosomes. If not, another explanation could be that the haemosiderin and the siderosomal ferritin were inadvertently isolated from

different liver cell types (hepatocytes and sinusoidal cells). Different cell types might acquire siderosomal phosphate from different sources [8] or might process iron dextran in different ways or at different rates.

MATERIALS & METHODS - See also chapter 2

Preparation of liver homogenate

The liver was cut into pieces and 0.15 M NaCl was added up to a concentration of 1 g of tissue/10 ml 0.15 M NaCl. Homogenization of the liver was performed in a Potter-Elvehjem homogenizer (500 rpm six complete strokes). One third of the homogenate was used for preparation of the cytosolic fraction and two-thirds were used for the preparation of the siderosomal fraction.

Preparation of the cytosolic fraction

This fraction was prepared according to de Duve et al. [9]. The homogenate was centrifuged for 110 min at 70,000 *g*, 4°C in a Beckman ultracentrifuge type L5-65, rotor 35. The supernatant representing the cytosolic fraction, was frozen at -20°C.

Preparation of the siderosomal fraction

Siderosomes were prepared according to Hultcrantz et al. [10] by the use of a continuous sucrose gradient (1.4-2.2 M) in a Beckman ultracentrifuge, rotor SW27. The pellet representing the siderosomal fraction, was resuspended in 0.3 M sucrose. Arylsulphatase (EC 3.1.6.1) activity was determined as described in chapter 2.

Chromatography

Gel filtration chromatography of the ferritins was performed on a Sepharose 6B column (4 cm × 91 cm) in 0.05M LiOH/borate buffer (pH 8.6). Fractions of 2.5 ml were collected and protein was monitored at 280 nm. Protein-containing fractions were pooled and half of the pool of fractions was dialysed against bidistilled water for 5 days.

REFERENCES

1. **Michaelis L, Coryell CD, Granick S** (1943) Ferritin: III The magnetic properties of ferritin and some other colloidal ferric compounds. J Biol Chem 148:463-480
2. **Myagkaya GC, de Bruijn WC** (1982) X-ray microanalysis of cellular localization of ferritin in mammalian spleen and liver. Micron 13:7-21
3. **Treffry A, Harrison PM, Cleton MI, de Bruijn WC, Mann S** (1987) A note on the composition and properties of the ferritin iron cores. J Inorg Biochem 31:1-6
4. **Andrews SC, Brady MC, Treffry A, Williams JM, Mann S, Cleton MI, de Bruijn WC, Harrison PM** (1988) Studies on haemosiderin and ferritin from iron-loaded rat liver. Biol Metals 1:33-42
5. **Cleton MI, Frenkel EJ, de Bruijn WC, Marx JJM** (1986) Determination of iron to phosphorus ratios of iron storage compounds in patients with iron overload: a chemical and electron probe X-ray microanalysis. Hepatology 5:848-851
6. **Cleton MI, de Bruijn WC, van Blokland WTM, Marx JJM, Roelofs JM, Rademakers LHPM** (1988) Iron content and acid phosphatase activity in hepatic parenchymal siderosomes of patients with hemochromatosis before and after phlebotomy treatment. Ultrastruc Pathol 12:161-174
7. **Treffry A, Harrison PM** (1978) Incorporation and release of inorganic phosphate in horse spleen ferritin. Biochem J 171:313-320
8. **Weir MP, Gibson JF, Peters TJ** (1984) Biochemical studies on the isolation and characterization of human spleen haemosiderin. Biochem J 223:31-38
9. **de Duve C, Pressman BC, Gianetto R, Wattiaux R, Appelmans F** (1955) Intracellular distribution patterns of enzymes in rat liver tissue. Biochem J 60:604-617
10. **Hultcrantz R, Glaumann H** (1982) Studies on the rat liver following iron overload. Biochemical studies following iron mobilization. Lab Invest 46:383-393

CHAPTER 4

CYTOSOLIC AND SIDEROSOMAL FERRITINS

Morphology and image analysis

SUMMARY

Four ferritin fractions obtained by chromatography (chapter 3) were examined with the electron microscope. Using image analysis, mean iron-core diameters were determined. Comparison of the mean iron-core diameter of the major cytosolic fraction, CMF, and the major siderosomal fraction, SVVF, shows the ferritin in the siderosomes to have the largest mean iron-core diameter. However, image analysis and morphology also showed that the diameters of the individual iron particles that are present in the SVVF fraction, diverged more widely than those found in CMF. Moreover, the SVVF iron particles are found to form aggregates with large particles of iron-deficient material, that is also present in the CVVF and the SMF fraction.

The cytosolic and siderosomal ferritins described in chapter 3 were further analysed to establish immunological and morphological differences and to determine whether they resemble haemosiderin. The morphological and element specific analyses on the ferritin fractions were performed using electron spectroscopy and image analysis.

RESULTS

Immunological identification

Protein concentrations of cytosolic and siderosomal fractions used for immunological identification were as follows: 1.25 g/l (CMF), 0.75 g/l (CVVF), 0.50 g/l (SMF) and 2.00 g/l (SVVF).

All four fractions formed one single precipitin line in the Ouchterlony immunodiffusion assay against specific antiserum. Although the line formed by the SVVF was weak, it merged completely with the single line produced by the material from the CMF.

Morphology

The morphology of each fraction was examined by electron spectroscopy. Zero-loss images of the four fractions are presented in Figure 4.1. These images showed that all fractions, except for the CMF, contain two kinds of electron dense particles of which the smaller ones resemble ferritin. EELS revealed that the smaller particles indeed contain iron (see spectra under images), whereas the larger particles do not. Element-specific, (semi-) net-intensity iron images corresponded with ESI zero-loss images with respect to the localization of the ferritin-like particles, but not with respect to the size of the particles (CMF, Figure 4.2A,B).

The mean size $\pm$ SD, mode and range of the ferritin cores as calculated from the zero-loss images by IBAS are summarized in Table 4.1.

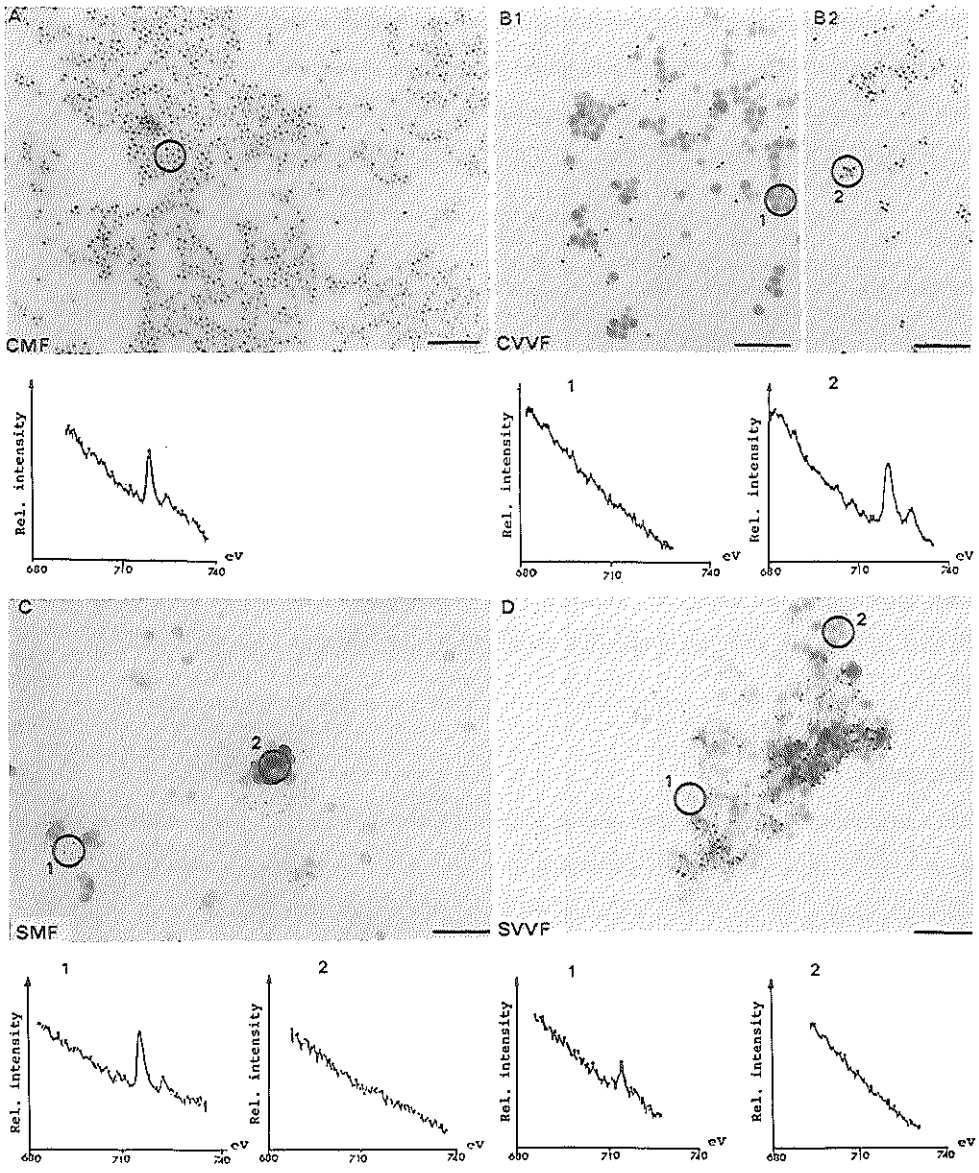

Figure 4.1

Zero-loss images and electron energy-loss spectra of the isolated products. Energy loss (x-axis) is plotted against relative intensity (y-axis). O=analysed area. Bar:100 nm

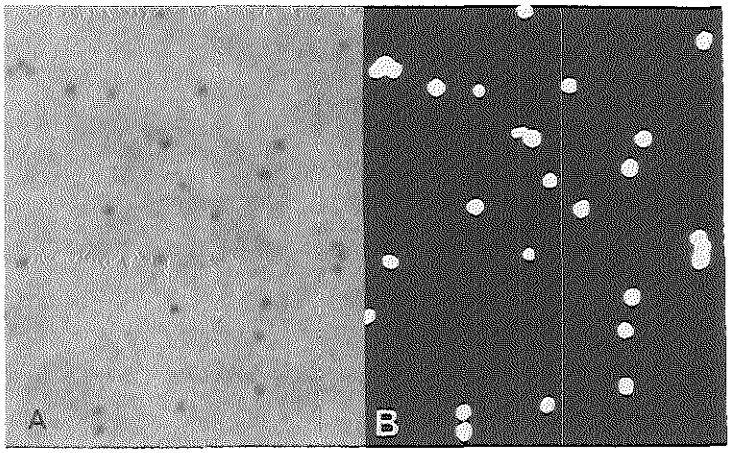

Figure 4.2

Zero-loss image (A) and element-specific image (B) of the CMF. The cores in the element-specific image are larger

Table 4.1

Iron core diameters from zero-loss images

Fraction	Diameter (nm)		
	mean $\pm$ SD	mode	range
CMF	5.8 $\pm$ 0.9	5.7	3.0
CVVF	5.8 $\pm$ 0.9	5.7	3.0
SMF	5.6 $\pm$ 1.0	4.3	3.8
SVVF	6.7 $\pm$ 1.3	7.2	6.4

DISCUSSION

Immuno double diffusion shows that the precipitin lines formed by CVVF and SVVF merge completely. Therefore, we can assume that these fractions are immunologically the identical. Regarding the fact that the SVVF shows a large absorbance peak at 280 nm (chapter 3), whereas it forms only a weak precipitin line in the Ouchterlony assay, two explanations are possible: (1) an additional protein must be present in this fraction or (2) the fraction consists of a protein that has lost almost all its ferritin epitopes and therefore cannot react with antiserum against rat liver ferritin. Explanation (2) is in line with the observations that (a) under iron-overload conditions, increased iron content in lysosomes/ siderosomes is not accompanied by increased immunoreactivity [1] and (b) that most of the particles in lysosomes/siderosomes that resemble ferritin iron cores represent ferritin iron cores divested of protein or cores which are surrounded by denatured protein [2]. Our morphological results provide evidence for explanation (1), as in all fractions, except in the case of the CMF, large particles of iron-deficient material are present. Preliminary studies show that the ferritin can be separated from this material by chromatography on a Sepharose 4B column.

Although previous work with ferritin in ultrathin sections found a good correlation between core size measurements on zero loss and element-specific images [3], this was not the case in this study, with air-dried ferritin preparations. The cores in the element-specific image were larger (Figure 4.2). As the zero-loss measurements on isolated cytosolic ferritin correlated well with our previous measurements on cytosolic ferritin in ultrathin sections, we used zero-loss images for core size determinations in this comparative study.

Mean iron-core diameters found for both cytosolic fractions (5.8 nm) are in line with earlier data [4]. Comparison of the mean iron-core diameter of the major cytosolic fraction, CMF, and the major siderosomal fraction, SVVF, shows that the mean iron-core diameter in the siderosomes is largest (6.7 nm). However, image analysis and morphology also show that the diameters of the individual iron particles that are present in the SVVF fraction, differ more widely than those found in CMF (range 6.4, Table

4.1). In short, SVVF seems to be a rather heterogeneous fraction. Although the SMF fraction elutes at a position similar to monomeric cytosolic ferritin (Figure 3.1), it frequently contains very small iron particles (mode 4.3 nm). Apparently, when incorporation into the siderosomes occurs, parts of the iron-containing cores of the ferritins are lost.

In conclusion, we can say that siderosomal ferritin has a larger iron-core diameter than cytosolic ferritin. In the previous chapter we saw that siderosomal ferritin contains less phosphorus than cytosolic ferritin. It is possible that these observations are somehow related.

MATERIALS & METHODS - See also chapter 2

Protein determination

Protein was determined according to Markwell et al.[5] at 660 nm.

REFERENCES

1. **Cooper PJ, Iancu TC, Ward RJ, Guttridge KM, Peters TJ** (1988) Quantitative analysis of immunogold labelling for ferritin in liver from control and iron-overloaded rats. Histochem J 20:499-509
2. **Richter GW** (1983) Cellular ferritin overload and formation of hemosiderin. In: Urishizaki I, Aisen Ph, Listowsky I, Drysdale JW (eds) Structure and function of iron storage and transport proteins I. Elsevier, Amsterdam, pp. 155-162
3. **Sorber CJW, van Dort JB, Ringeling PL, Cleton-Soeteman MI, de Bruijn WC** (1990) Quantitative energy-filtered image analysis in cytochemistry II. Morphometric analysis of element-distribution images. Ultramicroscopy 32:69-78
4. **Andrews SC, Brady MC, Treffry A, Williams JM, Mann S, Cleton MI, de Bruijn WC, Harrison PM** (1988) Studies on haemosiderin and ferritin from iron-loaded rat liver.

Biol Metal 1:33-42

5. **Markwell MAK, Haas SM, Bieber LL, Tolbert NE** (1978) A modification of the Lowry procedure to simplify protein determination in membrane and lipoprotein samples. Anal Biochem 193:265-275

CHAPTER 5

ANALYSIS OF IRON-CONTAINING COMPOUNDS IN DIFFERENT COMPARTMENTS OF THE RAT LIVER AFTER IRON-LOADING

SUMMARY

The livers of iron-loaded rats were fractionated and a cytosolic fraction, a lysosomal fraction, a siderosomal fraction and haemosiderin were obtained. All iron-containing compounds from these fractions were isolated and their morphology, Fe/P ratios, iron-core diameter and peptide content were compared. The cytosolic fraction contained ferritin (CF) and a slower sedimenting, light ferritin (CLF). The lysosomal fraction also contained ferritin (LF) and a slower sedimenting light ferritin (LLF). The siderosomal fraction contained ferritin (SF), a faster sedimenting non-ferritin iron compound (SIC) and haemosiderin (HS). SIC and HS did not resemble ferritin as much as the other products did, but were found to be water-insoluble aggregates. The Fe/P ratios of CF and CLF were lower than the Fe/P ratios of LF and LLF and these in turn had lower Fe/P ratios than SF, SIC and HS. The iron core diameter of the cytosolic ferritin was increased after lysosomal uptake. The iron core diameters of the siderosomal products were smaller. CLF, CF, LF, LLF and SF contained one kind of subunit of approximately 20.5 kDa. SIC and HS contained other peptides in addition to the 20.5 kDa subunit. The results indicate that storage of ferritin molecules is not limited to the cytosolic compartment, but also takes place in the lysosomes. However, extensive degradation of the ferritin molecule seems to be confined to the siderosomes.

In order to investigate a possible transition process, various studies of haemosiderin and ferritin have been performed, such as Mössbauer spectroscopic studies [1], iron release and uptake [2-4], the iron core composition and diameter [5,6] and peptide content [7,8]. Yet, it is still not entirely clear how and where a possible transition takes place [9-11]. Our previous chromatographic studies (chapter 3) in iron dextran treated rats have shown that dialysis had no effect on the Fe/P ratios of the major cytosolic and siderosomal fractions.

In this study, we fractionated the livers of similarly treated rats using a fractionation scheme that was based on the scheme of Richter [12]. This allowed us to isolate, besides haemosiderin, a cytosolic fraction, a lysosomal fraction and a siderosomal fraction in one procedure. From these fractions we isolated all iron-containing products. By comparing their iron and protein characteristics, we traced the processing of cytosolic ferritin in lysosomes and siderosomes.

RESULTS

Iron-compounds

Twenty rat livers from iron-loaded rats were pooled and fractionated. Figure 5.1 shows the fractionation scheme used which is described in chapter 2.

All intermediate and end products from the ferritin isolation scheme (Figure 5.2) were screened for the presence of iron-containing compounds. Water-soluble products were dissolved in 0.15 M NaCl and water-insoluble compounds were solubilized in 20 mM tetramethylammonium hydroxide.

From the cytosolic fraction, two iron-containing products were isolated, one "normal" ferritin end product (CF) and an intermediate product in the 78,000 *g* supernatant (Figure 5.2, sup II).

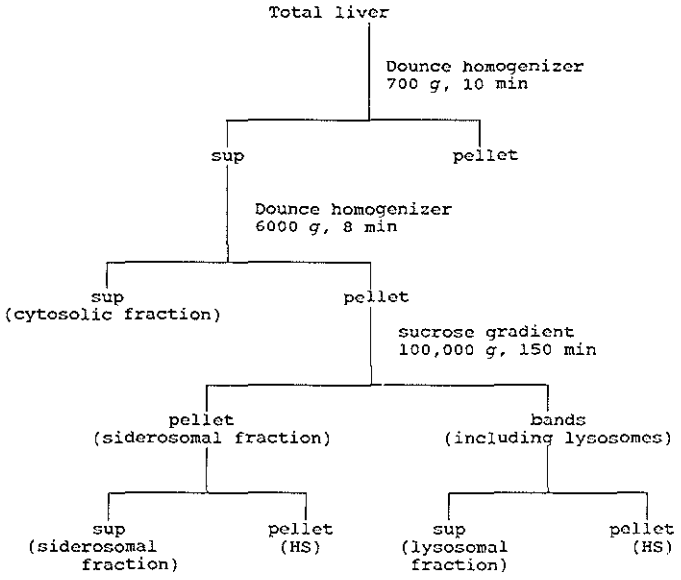

Figure 5.1
Fractionation scheme for the preparation of the cytosolic, the lysosomal and siderosomal fraction and the haemosiderin-containing fraction

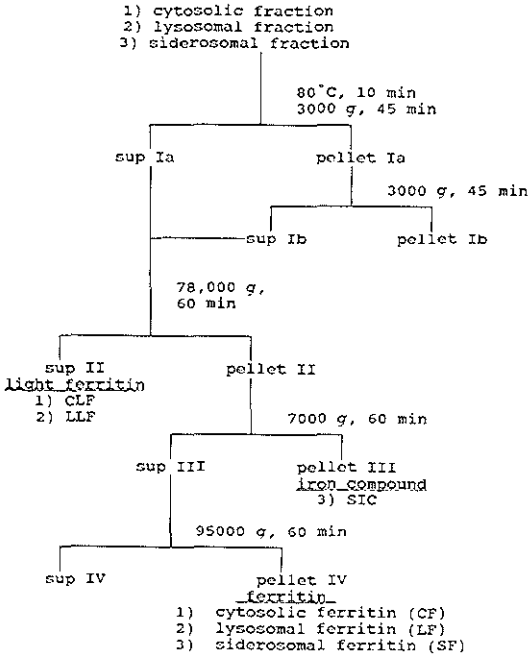

Figure 5.2
Ferritin isolation scheme

A similar result was obtained for the lysosomal fraction: a ferritin end product (LF) and an intermediate product in the 78,000 *g* supernatant (Figure 5.2, sup II). The siderosomal fraction also yielded two products: the "normal" ferritin end product (SF) and an intermediate product in the 7000 *g* pellet (Figure 5.2, pellet III). In addition to the haemosiderin (HS) isolated earlier (Figure 5.1), the end products and the intermediate products were tested in an Ouchterlony assay to determine their reaction with anti-(rat liver ferritin). Except for the haemosiderin and the intermediate product from the siderosomes, they all reacted with the antibody. Based on their positive reaction with specific antiserum we called the cytosolic intermediate product cytosolic light ferritin (CLF) and the lysosomal intermediate product lysosomal light ferritin (LLF). The siderosomal intermediate product was called siderosomal iron component (SIC). From CLF and LLF low-molecular-mass material was isolated by means of centrifugation at 95,000 *g*. The material found in the supernatant, proved to be ferritin-related (see Figure 5.6), and will be discussed in chapter 9.

Morphology

All products reacting with the anti-(rat liver ferritin) serum morphologically resembled ferritin: round particles lying in paracrystalline arrays as shown in the ESI micrographs of Figure 5.3. The SIC, which indeed contained iron as shown by the electron energy loss spectrum (Figure 5.4) morphologically resembled haemosiderin (Figure 5.3). Core size determinations of ferritins are presented in Table 5.1.

Fe/P ratios

The Fe/P mass ratios of the ferritins, the SIC and the haemosiderin as determined by EPMA are presented in Table 5.1.

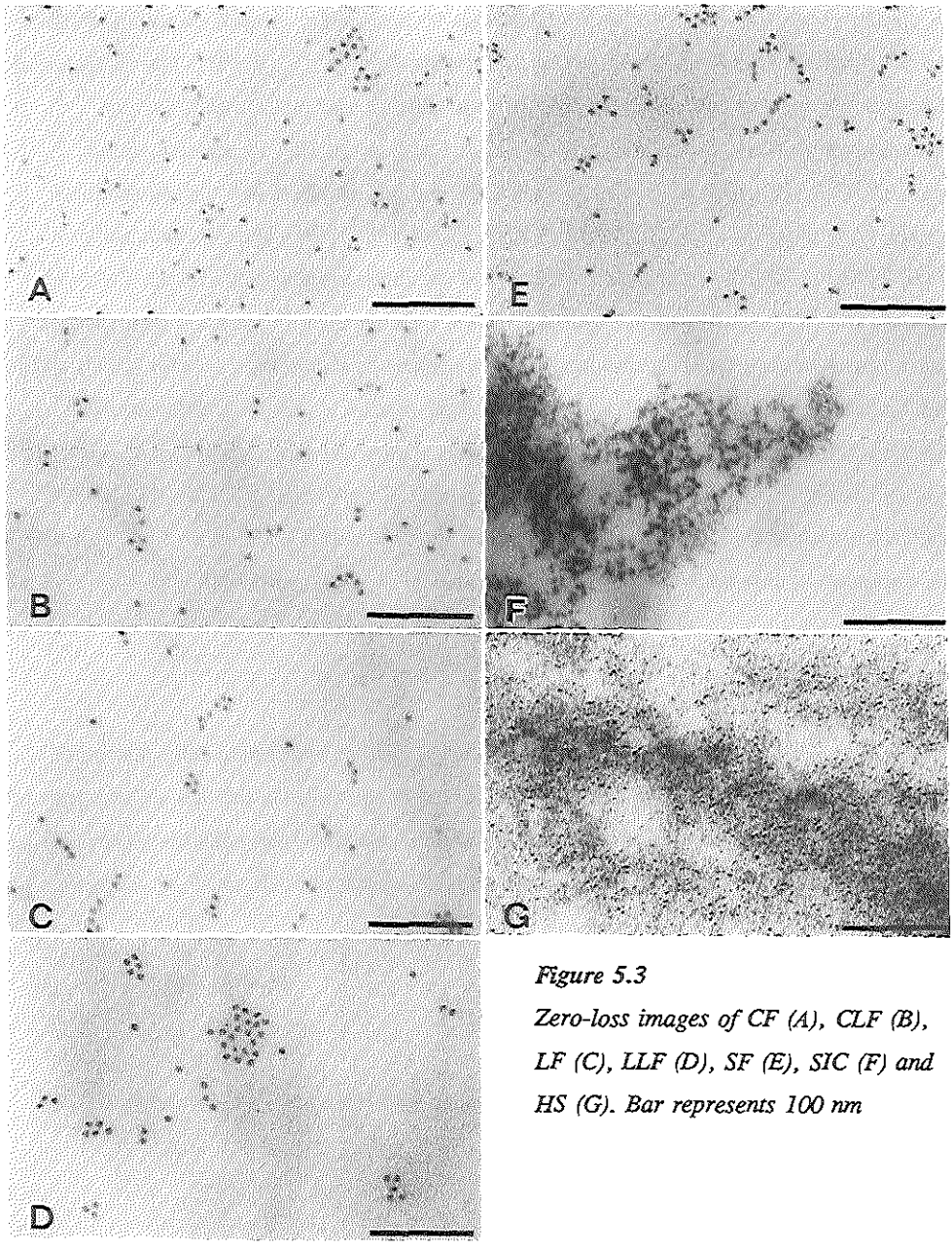

Figure 5.3
Zero-loss images of CF (A), CLF (B), LF (C), LLF (D), SF (E), SIC (F) and HS (G). Bar represents 100 nm

Figure 5.4

EELS of SIC with on the y-axis relative intensity and energy (eV) on the x-axis

Table 5.1

Iron core diameters (nm) and Fe/P ratios of all products

Fraction	*n*	Diameter	*p*	*n*	Fe/P	*p*
CLF	692	6.1 ± 0.6		10	5.5 ± 1.7	
			*			*
CF	170	6.9 ± 0.9		12	3.5 ± 0.8	
			*			*
LLF	3074	6.7 ± 0.8		10	4.9 ± 1.1	
			*			*
LF	709	7.6 ± 0.9		13	8.0 ± 4.0	
			*			n.s.
SF	544	7.2 ± 0.9		13	10.6 ± 3.6	
			n.d.			n.s.
SIC	-	<6		10	12.1 ± 2.8	
			n.d.			*
HS	-	<6		12	17.5 ± 3.4	

Results are the average ± SD; *n* = number of particles analysed by IBAS/ number of determinations by EPMA; n.d. = not determined; n.s. = not significant; * = $p < 0.05$ determined by Mann-Whitney *U*-test.

Ferritin iron-saturation

The amount of material available was only sufficient to calculate the number of iron atoms/ferritin molecule once. The results indicated that the iron saturation of the lysosomal ferritins was higher than that of the cytosolic ferritins. Siderosomal ferritin-iron content could not be determined.

Protein analysis

On a 5% polyacrylamide gel CF, CLF, LF, LLF and SF each showed one band with the same migration rate, staining positively for protein and iron. The low-molecular-mass material present in the supernatant of CLF and LLF also showed one band, but this band migrated much faster and stained positively for protein but negative for iron. HS and SIC did not migrate at all.

On a 15% SDS gel CF, CLF, LF, LLF, SF, SIC and HS showed a band at 20.5 kDa. In addition to this band SIC and (sometimes) HS also showed several bands in the region of 60-67 kDa and a band at 36 kDa. HS (always) showed an extra band at 14 kDa (Figure 5.5). The low-molecular-mass material in the supernatant of CLF and LLF showed one band at 14.4 kDa (not shown).

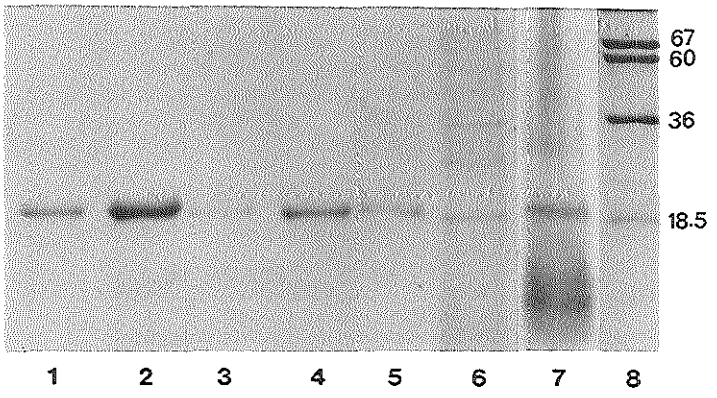

Figure 5.5 SDS-PAGE of CF (1), CLF (2), LLF (3), LF(4), SF(5), SIC (6), HS (7); HMW (marker)(8)

The 20.5-kDa bands of CF, CLF, LF and LLF and the 14.4-kDa band of the fast migrating material from CLF and LLF were positive in the Western blot (Figure 5.6). In the Western blot the 20.5-kDa subunit was found at 20-23 kDa, depending on the marker used. Immunoblotting with siderosomal products was not possible due to unavailability of material. Therefore, we used additional siderosomal material from fresh livers for the Western blot (Figure 5.7). SF shows many extra smaller and larger peptides along with the 20.5-kDa peptide (43-67 kDa, 20-25 kDa and 12 kDa). SIC contains the 20.5-kDa peptide and a peptide of 18 kDa. Haemosiderin reacted only faintly. CF and LF from fresh liver were used as a reference.

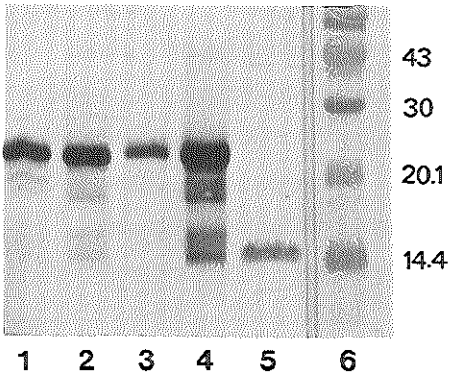

Figure 5.6
Western blot after SDS-PAGE of LLF (1) LF (2), CLF (3), CF (4), low molecular mass material (5); LMW (marker) (6)

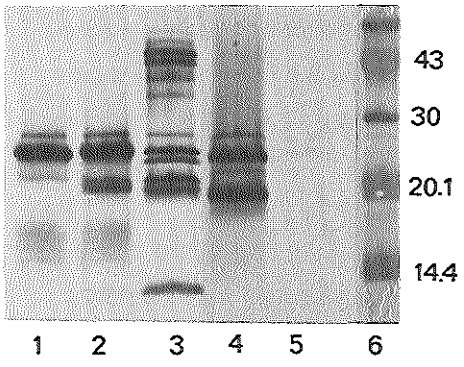

Figure 5.7
Western blot analysis after SDS-PAGE of material from fresh livers. CF (1), LF (2), SF (3), SIC (4), HS (5); LMW (marker) (6)

DISCUSSION

In chapter 3 we obtained a cytosolic and a siderosomal ferritin fraction which were subjected to gel filtration chromatography on Sepharose 6B. In chapter 4 it was shown that the main siderosomal fraction was highly heterogeneous, containing in addition to ferritin large particles of iron-deficient material. After chromatography on a Sepharose 4B column this fraction produced a fraction with an Fe/P ratio of 8:1 (unpublished). Moreover, the cytosolic fraction as used in the previous study displayed lysosomal enzyme activity, indicating a contamination with lysosomal material. In view of these data, we decided to switch to a more gentle fractionation technique [12] using the total liver homogenate before starting experiments with parenchymal cells versus sinusoidal cells. This technique allowed us not only to obtain a relatively pure cytosolic fraction, but also to separate the lighter (mainly ferritin containing) lysosomes from the heavily loaded (mainly haemosiderin containing) siderosomes. In this manner we obtained, in a single procedure, (a) a cytosolic fraction, (b) a lysosomal fraction, (c) a siderosomal fraction and (d) haemosiderin (Figure 5.1). From these fractions all iron-containing compounds were isolated (Figure 5.2) and compared with each other. The low-molecular-mass material was left out of the comparison because it did not contain the 20.5-kDa subunit. It will be further investigated in chapter 9.

Comparing the lysosomal products (LF and LLF, Figure 5.2) with the cytosolic products (CF and CLF, Figure 5.2) we can see that they have much in common. The conclusion that the products from these cellular compartments are ferritins would seem to be correct, as they (a) react with anti-(liver ferritin) antibodies, (b) are soluble in water, (c) contain a 20.5-kDa subunit reacting positively in the Western blot (Figure 5.6), and (d) resemble ferritin morphologically (Figure 5.3). However, the lysosomal products do differ from the cytosolic ferritins with respect to two parameters: iron-core size and Fe/P ratio, both of which are greater in the lysosomal ferritins (Table 5.1). Our morphometric data about the core size are in line with those from Iancu et al. [13] who observed a similar difference in size between cytosolic and lysosomal ferritin *in situ* in enterocytes from the small intestine of carbonyl-iron-loaded rats.

Preliminary biochemical results indicate that the iron content of our ferritins increases in parallel to the increase in iron core diameter. This would mean that lysosomal ferritin is still capable of taking up iron inside the lysosome. However, our biochemical data result from only one experiment. Besides, ferritin concentrations are calculated without taking into account the possible differences in immunological reactivity between cytosolic and lysosomal ferritins.

An increase in Fe/P ratio in the lysosomal ferritin indicates a (relative) increase in iron and/or a (relative) decrease in phosphorus. Protein analysis indicates that no changes occur in the protein coat after lysosomal uptake. Apparently, the first events that take place in the lysosomal compartment are the uptake and storage of ferritin without loss of its iron and without degradation of its protein coat.

Comparing the siderosomal products with the lysosomal products we see that they have less in common. Besides the siderosomal ferritin, two other products are present, i.e. the siderosomal iron compound (SIC) and the haemosiderin. Siderosomal ferritin resembles the other ferritin fraction with respect to solubility and immunoreactivity. Yet, there are some indications that its protein coat is different. As Figure 5.3 shows, the distances between its particles are less regular, and Figure 5.7 shows that its coat contains several peptides that are not found, to such an extent, in the other ferritins. Haemosiderin and SIC are water-insoluble. Although both contain the 20.5-kDa subunit, only SIC reacts with specific anti-(liver ferritin) antibodies. It is not likely that the SIC is iron dextran, because intracellular iron dextran disappears from the liver over a 2-week period following the iron-dextran injections [14,15]. All three siderosomal products differ from the lysosomal products in that their Fe/P ratio is increased and the iron core diameter is smaller.

Assuming that siderosomal ferritin originates from lysosomal ferritin the increase in Fe/P ratio with a simultaneous decrease in core diameter can only be explained by a heavy loss of phosphorus accompanied by or inducing a smaller loss of iron. This suggestion is supported by others [16] who found that phosphate is released more readily, and ahead of iron, from native ferritin. They suggested that much of the phosphate was located on core surface sites and is therefore lost as surface iron is lost.

SDS-PAGE (Figure 5.5) shows that all products are ferritin-related, as they all contain the 20.5-kDa subunit. In the Western blot, however, other ferritin-related peptides are also visible. These peptides are not visible in the cytosolic ferritin, faintly in the lysosomal ferritin, but they are clearly visible in the siderosomal ferritin. As is known from the literature [17] iron stabilizes the protein shell. A loss of iron, therefore, could lead to destabilisation of the ferritin protein shell. Another possibility is that, as soon as iron is lost from the core, the ferritin protein coat is degraded by an iron-catalysed Fenton reaction. This reaction is supposed to occur in the siderosomes and to be responsible for lipid peroxidation of the siderosomal membranes, causing a higher fragility of these membranes [18,19]. Both scenarios could explain why in the Western blot the 20.5-kDa subunit is found along with other peptides in the siderosomal products. Apparently, the siderosomal compartment is the site where the greatest changes to the ferritin molecule take place.

Thus, the processes which take place in the lysosomes and in the siderosomes differ. The lysosomes function as a site at which ferritin storage takes place, whereas the siderosomes function as a site of ferritin breakdown.

MATERIALS & METHODS - See also chapter 2

Instrumental conditions EPMA

Spot diameter:1μm; dwell time/determination:100 sec; tilt angle 18°;

REFERENCES

1. **Rimbert JN, Dumas F, Kellershohn C, Girot R, Brissot P** (1985) Mössbauer spectroscopy study of iron overloaded livers. Biochimie 67:663-668
2. **Harrison PM, Hoy TG, Macara IG, Hoare RJ** (1974) Ferritin iron uptake and release. Structure-function relationships. Biochem J 143:445-451
3. **Brady MC, Lilley KS, Treffry A, Harrison PM, Hider RC, Taylor PD** (1989) Release

of iron from ferritin molecules and their iron cores by 3-hydroxypyridonine chelators in vitro. J Inorg Biochem 35:9-22

4. **Biemond P, van Eijk HG, Swaak AJG, Koster JF** (1984) Iron mobilization from ferritin by superoxide derived from stimulated polymorphonuclear leucocytes. Possible mechanism in inflammation diseases. J Clin Invest 73:1576-1579
5. **Treffry A, Harrison PM, Cleton MI, de Bruijn WC, Mann S** (1987) A note on the composition and properties of the ferritin iron cores. J Inorg Biochem 31:1-6
6. **Andrews SC, Brady MC, Treffry A, Williams JM, Mann S, Cleton MI, Bruijn de WC, Harrison PM** (1988) Studies on haemosiderin and ferritin from iron-loaded rat liver. Biol Metal 1:33-42
7. **Weir MP, Gibson JF, Peters TJ** (1984) Biochemical studies on the isolation and characterization of human spleen haemosiderin. Biochem J 223:31-38
8. **Andrews SC, Treffry A, Harrison PM** (1987) Siderosomal ferritin. The missing link between ferritin and haemosiderin? Biochem J 245:439-446
9. **Hoy TG, Jacobs A** (1981) Ferritin polymers and the formation of haemosiderin. Br J Haematol 49:593-602
10. **Richter GW** (1986) Studies of iron overload. Lysosomal proteolysis of rat liver ferritin. Pathol Res Pract 181:159-167
11. **Cooper PJ, Iancu TC, Ward RJ, Guttridge KM, Peters TJ** (1988) Quantitative analysis of immunogold labelling for ferritin in liver from control and iron-overloaded rats. Histochem J 20:499-509
12. **Richter GW** (1984) Studies of iron overload. Rat liver siderosome ferritin. Lab Invest 50:26-35
13. **Iancu TC, Ward RJ, Peters TJ** (1987) Ultrastructural observations in the carbonyl iron-fed rat, an animal model for haemochromatosis. Virchows Arch B Cell Pathol 53:208-217
14. **de Bakker JM** (1983) On the origin of peritoneal resident macrophages. PhD thesis, University of Leiden
15. **Andrews SC, Treffry A, Harrison PM** (1988) Studies on the subcellular processing of iron dextran by rat liver. Biochem Soc Trans 16:854-855
16. **Treffry A, Harrison PM** (1978) Incorporation and release of inorganic phosphate in horse spleen ferritin. Biochem J 171:313-320
17. **Crichton RR** (1969) Studies on the structure of ferritin and apoferritin from horse spleen.

I. Tryptic digestion of ferritin and apoferritin. Biochim Biophys Acta 194:34-42

18. **Bacon BR, Britton RS** (1990) The pathology of hepatic iron overload: a free radical-mediated process? Hepatology 11:127-137

19. **Selden C, Owen M, Hopkins JMP, Peters TJ** (1980) Studies on the concentration and intracellular localization of iron proteins in liver biopsy specimens from patients with iron overload with special reference to their role in lysosomal disruption. Br J Haematol 44:593-603

CHAPTER 6

COMPARISON OF CYTOSOLIC PRODUCTS FORMED IN RAT LIVER IN RESPONSE TO PARENTERAL AND DIETARY IRON-LOADING

(A pilot study)

SUMMARY

Two different methods were used to induce a condition of iron overload in rats. One group of rats received injections of iron dextran and another group of rats received a carbonyl-iron-enriched diet. The ferritins present in the liver cytosol of these rats were isolated and compared. From each group two cytosolic products were isolated with the use of ultracentrifugation: a cytosolic ferritin fraction (CF) and a (slower sedimenting) light ferritin fraction (CLF). There were no differences with respect to the protein coat (subunit composition and amino acid analysis). Analysis of the iron core revealed that the two CF fractions were similar, whereas the two CLF fractions differed with respect to their iron contents and to the packing of their cores. The carbonyl CLF product contained less Fe atoms per molecule, which, moreover, seemed to be packed in a less compact manner.

In many laboratories research has been done in the field of haemochromatosis, especially in rat liver. Initially, iron overload in rats was created parenterally by injecting them with iron dextran [1-3]. Parenterally iron-loading is a rapid method of creating a condition of iron overload in rats. But iron overload in hereditary haemochromatosis is created orally and is a slow process. Therefore, in the past few years iron has also been administered through a carbonyl-iron-enriched diet [4,5] or a combination of both methods [6,7]. Although several studies have shown that these methods lead to a different subcellular distribution pattern of ferritins [8,9], the actual nature of these ferritins was not examined. Therefore, the aim of this pilot study is to determine whether different methods of iron loading also result in different kinds of cytosolic products.

RESULTS

Liver iron content

Figure 6.1 shows concentrations of non-haem iron per gram liver (dry weight) in parenterally loaded, orally-loaded and control rats. In both iron-loaded groups the liver non-haem iron content was increased in comparison with control rats. The liver iron-content of the rats fed on a carbonyl-iron diet increased by a factor of five, while that of the parenterally loaded rats increased by a factor of nine.

Cytosolic products

The two groups of rats yielded similar cytosolic products, i.e. cytosolic ferritin (CF) and cytosolic light ferritin (CLF) and, in the supernatant of the CLF fraction, a low-molecular-mass protein (see chapter 9). CF and CLF were purified further by gel filtration chromatography on Sephacryl S300 SF . In both groups the precipitin line from the light ferritin fused with the line from the ferritin in an Ouchterlony immuno diffusion assay. Table 6.1 shows the iron content of the ferritins and the light ferritins. The CF fraction from the carbonyl group and the CF fraction from the Imferon group contain a similar iron content. The CLF fractions of the two groups differ widely in iron content.

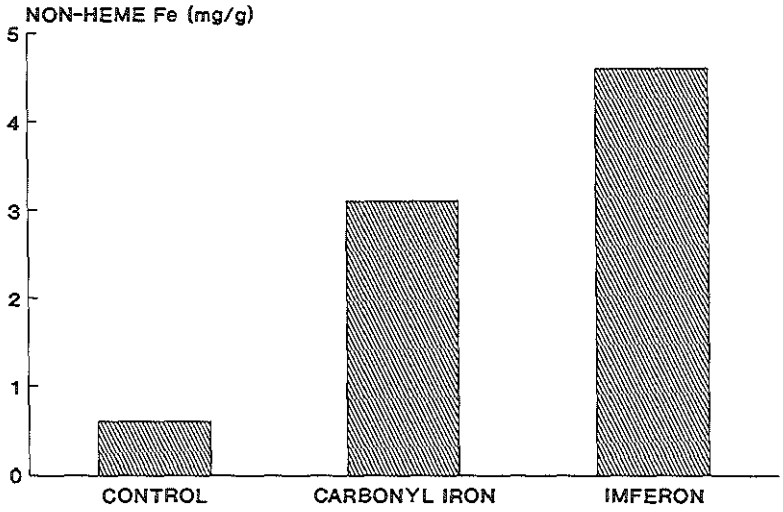

Figure 6.1

Liver non-haem iron content

Ultrastructural analysis

The ferritin and the light ferritin from the livers of the carbonyl-fed rats did not differ morphologically from the ferritin and the light ferritin isolated from the parenterally-loaded rats. Mean iron-core diameters obtained through image analysis are presented in Table 6.1.

Protein analysis

On a 4-30% gradient gel the ferritins and the light ferritins from the carbonyl-iron-fed rats and the Imferon-treated rats showed one band with an identical migration rate staining positively for protein and iron at a position of approximately 500 kDa. In Western blot analysis this band was recognized by anti-(rat liver ferritin) antiserum. Western blot analysis after SDS-PAGE on an 18% gel showed similar results for the Imferon-treated rats and the carbonyl-fed rats, i.e. a 20 kDa-band, both for the ferritins and the light ferritins.

Table 6.1

Iron content (number of Fe atoms) and iron-core diameter

		Fe atoms	Diameter (nm)
CF	Imferon	2456 ± 133	6.9 ± 0.9
	Carbonyl	2577 ± 185	6.8 ± 1.2
CLF	Imferon	2548 ± 391	6.1 ± 1.6
	Carbonyl	1009 ± 107	6.9 ± 1.2

Amino acid analysis

The amino acid compositions of the two ferritins were compared and are presented in Figure 6.2. Cysteine and proline were not determined. The $S\Delta Q$ value for the ferritins is 6.

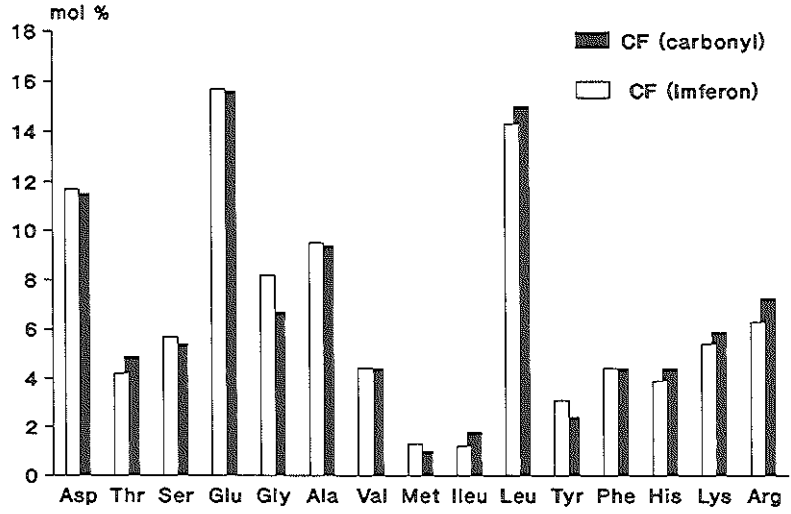

Figure 6.2

Amino acid composition of the CF fractions from both experimental groups

DISCUSSION

In this pilot study we compare the cytosolic products present in rats after parenteral and dietary iron-loading. In both iron-loading models similar cytosolic products (CF and CLF) are obtained. These products are immunologically identical, and consist of similar subunits. The low $S\Delta Q$ values of the CF products indicate that they have similar amino acid composition. Therefore, we may conclude that they have similar protein coats.
With regard to the iron part of the ferritins, our results are in agreement with other data [6,7,10] which show that a lower non-haem iron content of the liver does not result in less iron atoms per ferritin molecule. However, in these studies no attention was paid to light ferritin fractions. The results of this pilot study indicate that the lower liver non-haem iron content of the carbonyl-fed rat could be explained by the lower iron content of the light ferritin. The fact that the CLF fraction from the carbonyl group contains less iron than the CF fraction from this group suggests that, in this more gradual process of iron-loading, iron is incorporated in newly synthesized ferritin molecules, as soon as ferritin molecules contain approximately 2500 Fe atoms.
Our ultrastructural data (Table 6.1) indicate that the mean iron-core diameter in the CLF fraction from the carbonyl-fed rats is as large as the mean iron-core diameter in the two CF fractions, whereas our biochemical data show that the two CF fractions contain more than twice as many Fe atoms. Apparently, the iron core diameter gives only information about the packing of the core and not about the iron content of ferritin. This would mean that the carbonyl CLF core is less compact than the cores of the other products.

MATERIALS & METHODS - See also chapter 2

Animals

Two groups of rats were used. One group (n=2) received carbonyl iron, the other group (n=2) received iron dextran (Imferon^R).

REFERENCES

1. **van Wijk CP, Linder-Horowitz M, Munro HN** (1971) Effect of iron-loading on non-heme iron compounds in different liver cell populations. J Biol Chem 246:1025-1031
2. **Treffry A, Lee PJ, Harrison PM** (1984) Iron-induced changes in rat liver isoferritins. Biochem J 220:717-222
3. **Andrews SC, Treffry A, Harrison PM** (1987) Siderosomal ferritin. The missing link between ferritin and haemosiderin? Biochem J 245:439-446
4. **Iancu TC, Ward RJ, Peters TJ** (1987) Ultrastructural observations in the carbonyl iron-fed rat, an animal model for hemochromatosis. Virchows Arch B 53:208-217
5. **Britton RS, O'Neill R, Bacon BR** (1990) Hepatic mitochondrial malondialdehyde metabolism in rats with chronic iron overload. Hepatology 11:93-97
6. **Cleton MI, Mostert LJ, Sorber LWJ, de Jong AAW, de Jeu-Jaspars CMH, de Bruijn WC** (1989) Effect of phlebotomy on the ferritin iron content in the rat liver as determined morphometrically with the use of electron energy loss spectroscopy. Cell Tiss Res 256:601-605
7. **Mostert LJ, Cleton MI, de Bruijn WC, Koster JF, van Eijk HG** (1989) Studies on ferritin in rat liver and spleen during repeated phlebotomy. Int J Biochem 21:39-47
8. **Fletcher LM, Roberts FD, Irving MG, Powell LW, Halliday JW** (1989) Effects of iron loading on free radical scavenging enzymes and lipid peroxidation in rat liver. Gastroenterology 97:1011-1018
9. **Bacon BR, Tavill AS, Brittenham GM, Park CH, Recknagel RO** (1983) Hepatic lipid peroxidation in vivo in rats with chronic iron overload. J Clin Invest 71:429-439
10. **Richter GW** (1983) Cellular ferritin overload and formation of hemosiderin. In: Urishizaki I, Aisen Ph, Listowsky I, Drysdale JW (eds) Structure and function of iron storage and transport proteins I. Elsevier, Amsterdam, pp. 155-162

CHAPTER 7

EXPERIMENTS WITH PARENCHYMAL AND NONPARENCHYMAL CELLS FROM IRON-LOADED RATS

SUMMARY

The aim of the study was to investigate the notion that lysosomes and siderosomes of Kupffer cells, being macrophages, contain ferritin and haemosiderin from other sources, perhaps with other characteristics, than the lysosomes and siderosomes of hepatocytes. We hoped to fractionate parenchymal cells (hepatocytes) and sinusoidal cells (Kupffer and endothelial cells) isolated from the same (pooled) iron-loaded rat livers. As sinusoidal cells had taken up iron, their density had changed and the difference in sedimentation rate between parenchymal cells and sinusoidal cells had disappeared. Therefore, cells could not be separated using standard methods. Alternatively, hepatocytes and sinusoidal cells were isolated via enzyme perfusions, from separate iron-loaded rat livers.

We succeeded in fractionating the hepatocytes, but only the cytosolic fraction yielded enough ferritin to be analysed. Our attempt to fractionate the sinusoidal cells, using the detergens digitonin, was unsuccessful.

We concluded that the efficiency of this method was too low to compare lysosomal and siderosomal compounds present in parenchymal cells with those present in sinusoidal cells of the rat liver.

The liver consists mainly of two cell populations: parenchymal cells (hepatocytes) and sinusoidal cells (Kupffer and endothelial cells). When we used the whole liver in our previous experiments, we were working with a cytosolic, a lysosomal and a siderosomal fraction that were derived from a mixed cell population. Kupffer cells, after all, are macrophages, which phagocyte a whole range of compounds from circulation (including senescent erythrocytes), which are incorporated in their lysosomes for degradation [1]. This is why their lysosomes and siderosomes in particular might contain iron from various sources. Therefore, we preferred to separate siderotic rat livers into two populations: hepatocytes and sinusoidal cells, and analyse the iron-containing compounds present in these cells after fractionation.

RESULTS

HEPATOCYTES

Iron-compounds

Hepatocytes were isolated from the livers of 30 iron-loaded rats. The hepatocytes were pooled and fractionated into a cytosolic, a lysosomal and a siderosomal fraction, in the presence of the protease inhibitor PMSF. From the cytosolic fraction a ferritin (CF) and a light ferritin (CLF) were isolated. The supernatant of the CLF contained the ferritin-related low-molecular-mass protein that was also found in whole liver preparations (chapter 5). In addition, a few microlitres lysosomal ferritin and a few microliters haemosiderin were isolated from the other fractions. This low yield forced us to restrict our experiments to CF and CLF.

Electrophoresis

Native gel electrophoresis showed that CF and CLF had a molecular mass of approximately 500 kDa. SDS-PAGE showed that they consisted of peptides of

approximately 20.5 kDa, which were recognized by anti-(rat liver ferritin) antiserum.

Amino acid analysis

In Table 7.1 hepatic and whole liver CF are compared. The $S\Delta Q$ value is 177.

Electron microscopy

CF and CLF morphologically resembled cytosolic ferritin from whole liver preparations. Image analysis showed that the mean iron-core diameter of CF was 6.1 nm $\pm$ 0.8.

Table 7.1

Amino acid analysis of CF from whole liver and from hepatocytes

mol %	Liver	Hepatocytes	Δ^2
Asp	11.7	10.3	1.96
Thr	4.2	4.0	0.04
Ser	5.7	5.8	0.01
Glu	15.7	13.5	4.84
Gly	8.2	6.8	1.96
Ala	9.5	7.9	2.56
Val	4.4	4.3	0.01
Met	1.3	1.4	0.01
Ileu	1.2	1.7	0.25
Leu	14.3	11.6	7.29
Tyr	3.1	2.3	0.64
Phe	4.4	3.4	1.00
His	3.9	3.3	0.36
Lys	5.4	17.9	156.25
Arg	6.3	5.8	0.25
			$S\Delta Q$=177.43

SINUSOIDAL CELLS

Sinusoidal cells (Kupffer cells and endothelial cells) were isolated from the livers of 40 iron-loaded rats. As there is very little literature on the fractionation of iron-loaded sinusoidal cells [2], we tried several techniques: homogenization, Parr pressure bomb, ultrasonic treatment and osmotic shock. The effect, however, was either that the whole cell was ruptured or that the cell remained intact. Therefore, we tried to fractionate the cells using the detergent digitonin. Our aim was to rupture the cellular membrane, without affecting the lysosomal integrity.

Our first experiments, carried out on thawed cells, were used to establish the concentration of digitonin necessary to rupture the lysosomal membrane. Results looked promising, but thawed cells proved to be inconvenient for LDH assays. Our best result with fresh cells is shown in Figure 7.1. Plasma membrane and lysosomal membrane are virtually simultaneously ruptured. When 80% of the lactate dehydrogenase activity is released, 60% of the acid phosphatase is also released.

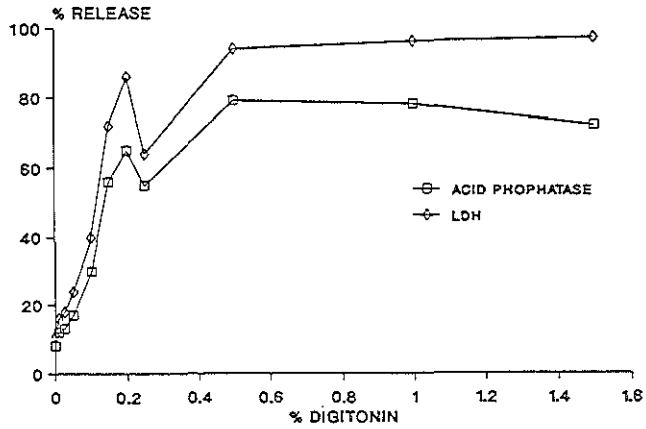

Figure 7.1

Release of lactate dehydrogenase (◇) and acid phosphatase (□) after incubation of hepatocytes with various concentrations digitonin.

DISCUSSION

Our aim was to separate the different cell types of the liver, to fractionate them into a cytosolic, a lysosomal and a siderosomal fraction, and to isolate the iron-compounds from these fractions, a procedure analogous to that followed for the whole liver. Unfortunately, the cells were difficult to separate, because they contained various amounts of iron. As a result of this variation, common separation procedures could not be applied and it was not possible to isolate both cell types from the same liver. Efficiency of the fractionation was very low and therefore, only the cytosolic fraction of the hepatocytes yielded enough ferritin. Results for hepatocytes are similar to the results obtained for whole liver preparations. This can be explained by the fact that hepatocytes contain most of the cytoplasm of the whole liver [3], and our method for creating a condition of iron overload is such that most of the ferritin is present in the cytosol. The lysosomes and siderosomes, in which we expected to find the greatest differences when the cell types were compared, could not be analysed. Fractionation of sinusoidal cells posed a further problem, especially in the case of Kupffer cells, with their highly-flexible plasma membrane. Perhaps a shorter period of incubation with digitonin, to prevent it from reaching the lysosomal membrane, would have yielded better results [4].
We are forced to conclude that the fractionation of sinusoidal cells was not a success. We did succeed in fractionating the hepatocytes, but only gathered enough material to look at the cytosolic fraction. All together, it seems that this technique for studying differences between lysosomal and siderosomal compounds from hepatocytes and sinusoidal cells is not to be recommended, in view of its lack of efficiency.

MATERIALS & METHODS

See chapter 2

REFERENCES

1. **Wardle EN** (1987) Kupffer cells and their function. Review article. Liver 7:63-75
2. **van Wijk CP, Linder-Horowitz M, Munro HN** (1971) Effect of iron loading on non-haem iron compounds in different liver cell populations. J Biol Chem 246:1025-1031
3. **Blouin A, Bolender RP, Weibel ER** (1977) Distribution of organelles and membranes between hepatocytes and nonhepatocytes in the rat liver parenchyma. A stereological study. J Cell Biol 72:441-455
4. **Hjelmeland LM, Chrambach A** (1984) Solubilization of functional membrane proteins. Methods Enzymol 104:305-319

CHAPTER 8

COMPARISON OF FERRITINS AND LIGHT FERRITINS FROM RAT LIVER CYTOSOL

SUMMARY

We compared cytosolic ferritins (CF) and light ferritins (CLF) isolated from the livers of a group of parenterally iron-loaded rats to determine whether the lower sedimentation rate of CLF might be caused by a lower iron content. The livers were not pooled to enable the detection of individual differences. In addition, using a different group of rats, we examined whether iron was mobilized from both CF and CLF following a resting period in excess of 4 weeks.

Our results show that the difference in sedimentation rate between CF and CLF cannot always be explained by a difference in iron content alone, there are other elements in the core which must contribute to this. Furthermore, upon a resting period, both CF and CLF seem to lose iron from their cores, without any apparent degradation of the ferritin molecule.

During the process of isolating ferritin, we came across a ferritin fraction that did not precipitate at 78,000 *g* after 60 min centrifugation. This fraction, which we called "light ferritin", was present in cytosolic and in lysosomal fractions (chapter 5). Since it is generally known that ferritin heterogeneity can be explained by difference in iron content [1], we assumed that the light ferritin was a ferritin fraction with a lower iron content than the "normal" ferritin fraction, which precipitates at 78,000 *g* after centrifugation for 60 minutes. However, in our pilot study on parenteral and dietary iron-loading (chapter 6), there seemed to be no difference in iron content between the CF and CLF of the parenterally iron-loaded rats (Table 6.1). As these experiments were carried out with (two) pooled livers, we did not know whether the values for separate livers differed widely, and whether extreme values were involved.
Therefore, in this chapter the focus is on ferritins and light ferritins isolated from the livers of parenterally iron-loaded rats. Two groups of (seven) rats were involved. One group was treated in the usual way, i.e. after the last iron-dextran injection, the rats received no further treatment for 4 weeks (resting period). We compared them to another group of seven rats for which the resting period was 16 weeks, as we were also interested in possible differences in the rate at which iron was mobilized from the core. Livers were not pooled to enable the detection of individual differences.

RESULTS

Liver non-haem iron content

Table 8.1 shows concentrations of non-haem iron per g liver (dry weight) in livers from rats which had a resting period of 4 weeks (rats 1-7), of 16 weeks (rats 8-14) and in livers from control rats (rats 15-17).

Ferritin iron-content

The livers were fractionated and light ferritin (CLF) and ferritin (CF) were isolated from the cytosolic fractions. The purity of the isolated products was checked on a 4-30% polyacrylamide gradient gel and in Ouchterlony assays against anti-(rat liver ferritin)

antibodies and anti-(rat liver) serum. After the determination of iron and protein concentrations of the products, we were able to calculate the iron content (Table 8.2). Data from Table 8.2 were used to calculate the mean iron-content of CF and CLF after a resting period of 4 and 16 weeks (Table 8.3). The results are twofold. First, considering the mean iron-content of CF and CLF within one group of seven rats, there is a significant difference between CF and CLF after a resting period of 4 weeks. Secondly, the mean iron-content of CF after a resting period of 16 weeks is significantly lower than after a resting period of 4 weeks. This also applies to CLF.

Table 8.1

Non-haem iron content of the livers. Resting period 4 weeks (rats 1-7), 16 weeks (rats 8-14) and control rats (rats 15-17)

4 weeks		16 weeks		Control	
Rat No.	mg Fe/g dry weight	Rat No.	mg Fe/g dry weight	Rat No.	mg Fe/g dry weight
1	5.6	8	4.7	15	0.4
2	19.3‡	9	3.9	16	0.6
3	4.7	10	2.9	17	0.8
4	5.5	11	2.8		
5	6.3	12	3.9		
6	4.4	13	3.6		
7	5.9	14	4.2		
(5.4 ± 0.7)¶		(3.7 ± 0.7)¶		(0.6 ± 0.2)¶	

¶Figures in parentheses represent mean ± SD
‡On the basis of the Dixon test for extreme values [2-4] this value was excluded from the calculation of the mean.

Table 8.2
Iron content of CF and CLF[‡]

Resting period	Rat no.	Fe atoms per CF molecule	Fe atoms per CLF molecule
4 weeks	1	1596	1621
	2	2710	1684
	3	1828	1503
	4	2079	1868
	5	1957	1805
	6	2308	2043
	7	2327	1828
16 weeks	8	1837	1505
	9	1869	1292
	10	1556	1148
	11	1688	1581
	12	1565	1490
	13	1755	1594
	14	3018	1846

[‡]Result of one determination in duplo

DISCUSSION

This study was carried out to determine whether the lower sedimentation rate of CLF could be caused by a lower iron content. In addition, we investigated whether iron was mobilized from both CF and CLF given a resting period longer than 4 weeks.
The results described above show that there is a great individual variability (Table 8.2) and that the difference in sedimentation rate between CF and CLF cannot always be explained by a difference in iron content. Table 8.2 shows, for instance, that in the group of the rats that had a resting period of 4 weeks, there is a CF molecule (rat 3) with

Table 8.3

Mean iron content (MIC) of CF and CLF

Fraction	Resting period (weeks)	Rat No.	MIC ± SD	Mann-Whitney *U*-test *p*-value	
				(a)	(d)
CF	4	1-7	2115 ± 368 (a)		
CLF	4	1-7	1765 ± 178 (b)	(b) *	*
CF‡	16	8-13	1712 ± 133 (c)	(c) *	n.s.
CLF	16	8-14	1494 ± 224 (d)		

‡On the basis of the Dixon test for extreme values [2-4], the value of rat no. 14 was excluded from the calculation of the mean; * = $p < 0.05$; n.s. = not significant

1828 Fe atoms, but also a CLF molecule (rat 7). Moreover, it shows that a molecule with 2043 iron atoms can be a CLF molecule (rat 6), whereas there are CF molecules with less Fe atoms (rats 1,3,5). Only if the results of rats 1-7 are pooled to calculate mean iron contents for CF and CLF (Table 8.3), is the iron content of CF significantly higher. This significant difference in mean iron-content between CF and CLF is not found in the group with a resting period of 16 weeks. Therefore, certainly after the resting period, iron content cannot explain the difference in sedimentation rate between CF and CLF. If it cannot be attributed to iron, the difference in sedimentation rate must therefore be caused by the other elements in the ferritin core, i.e. phosphorus, oxygen and hydrogen. Much attention has been paid to iron/phosphorus ratios. However, the formula for horse spleen ferritin, $(FeOOH)_8(FeO\text{-}OPO_3H_2)$, indicates that, in general, ferritin could contain considerable amounts of oxygen. Therefore, iron/oxygen ratios deserve at least as much attention as iron/phosphorus ratios.

After a resting period of 16 weeks, not only is the mean non-haem iron content of the liver (Table 8.1) decreased, but also the mean iron-contents of CF and CLF (Table 8.3, rats 8-14). Apparently, iron is mobilized from both ferritin fractions during the resting period of 16 weeks.

Recent publications [5] have shown that the iron content of ferritin does not change as a result of phlebotomy, although the non-haem iron content of the liver decreases. Therefore, it was concluded that when there is a demand for iron, the whole ferritin molecule is degraded. Our results indicate that this only applies to situations in which iron has to be mobilized very quickly. Otherwise, the iron is released from ferritin without degradation of the molecule.

MATERIALS & METHODS

See chapter 2

REFERENCES

1. **Bomford A, Berger M, Lis Y, Williams R** (1978) The iron content of human liver and spleen isoferritins correlates with their isoelectric point and subunit composition. Biochem Biophys Res Commun 83:334-341
2. **Dixon WJ** (1950) Analysis of extreme values. Ann Math Stat XXI:488-506
3. **Dixon WJ** (1951) Ratios involving extreme values. Ann Math Stat XXII:68-78
4. **de Jonge H** (1960) Inleiding tot de medische statistiek, deel 2, pp. 408-410
5. **Mostert LJ, Cleton MI, de Bruijn WC, Koster, JF, van Eijk HG** (1989) Studies on ferritin in rat liver and spleen during repeated phlebotomy. Int J Biochem 21:39-47

CHAPTER 9

PARTIAL CHARACTERIZATION OF A LOW-MOLECULAR-MASS PROTEIN PRESENT IN RAT LIVER

SUMMARY

The aim of the study was to investigate whether the low-molecular-mass protein present in the cytosolic fraction of all our preparations, and yielding a 14.4-kDa peptide after SDS-PAGE, could be a "building block" of ferritin. It proves to be a 40-kDa protein (p*I* about 8.6) which is recognized by anti-(rat liver ferritin) antibodies. Although it seems to be related to ferritin, its origin remains obscure, since it could not be characterized completely.

During the isolation of ferritins from livers of iron-loaded rats (chapter 5) we came across the light ferritin supernatant of the cytosolic and the lysosomal fractions. It proved to contain a protein that in SDS-PAGE yielded a 14.4-kDa peptide reacting with anti-(rat liver ferritin) antibodies. As the protein did not seem to contain iron, we did not pay much attention to it. However, the protein was also found in other preparations, with and without the protease inhibitor PMSF. Therefore, we decided to characterize the protein and investigate whether it could be a "building block" of ferritin.

RESULTS

Molecular mass determination

We initially attempted to determine the molecular mass of the native protein on polyacrylamide gels, but we were not able to find a protein that was recognized by anti-(rat liver ferritin) antibodies. Therefore, the supernatant of the light ferritin was subjected to gel filtration chromatography on Sephacryl S300 SF. The chromatogram showed a number of peaks. The fractions corresponding to the various peaks were run on SDS-gel and examined by Western blot analysis. The 14.4-kDa peptide was the only peptide that was recognized by the antibodies. It was present in fraction 36, corresponding to a molecular mass of approximately 40 kDa.

Subsequently, fraction 36 was run on a 12% native gel, followed by Western blot analysis. Although the gel showed a protein band at approximately 43 kDa, the Western blot showed no hybridization.

Isoelectric focusing and titration curve analysis

Fraction 36 showed two curves upon titration, indicating the presence of a rather basic protein (about p*I* 9) and an acidic protein (about p*I* 5). Isoelectric focusing showed several peptides, but the peptides at p*I* 5.2 and 8.6 were most prominent.

Amino acid analysis

At first, the acidic and the basic protein were isolated for amino acid analysis (Table 9.1) using preparative isoelectric focusing. This was only successful in the case of the acidic protein. The basic protein had to be hydrolysed while still in the agarose gel slice. To estimate the relatedness of basic proteins from various fractions (whole liver cytosol and lysosomes and hepatic cytosol) with each other and with rat liver L-subunit, $S\Delta Q$ values were calculated (Table 9.2).

Immunoreactivity

Ouchterlony assays and Western blot analyses of titration curves and isoelectric focusing experiments showed that the acidic protein was not recognized by antibodies, whereas the basic protein was.

DISCUSSION

The supernatant of the light ferritin proves to contain a number of proteins. Using gel filtration chromatography, it can be determined that a protein of 40-43 kDa is responsible for the 14.4-kDa peptide.

Isoelectric focusing shows that the peptide has a p*I* of about 8.6. This explains why the protein cannot be detected on native gels: at pH 8.3 the protein is positively charged and, therefore, will not migrate on gel. The protein which is visible on the 12% native gel at 43 kDa must be the acidic protein (p*I* 5) that is not recognized by anti-(rat liver ferritin) antibodies.

Since the basic protein cannot be eluted from the agarose gel slices after preparative focusing, we are not able to isolate the protein for further analysis.

Amino acid analysis - virtually the only course of action we can take - shows that the basic proteins resemble each other, whereas they do not resemble the L-subunit ($S\Delta Q$ value over 300).

Table 9.1

Amino acid composition of the basic proteins from different fractions

mol%	Cytosol	Lysosomes	Hepatocytes	L-subunit‡
Asp	7.4	7.5	8.4	12.2
Thr	5.2	4.8	1.9	4.3
Ser	11.5	9.8	7.4	5.5
Glu	10.2	10.8	10.0	15.2
Gly	17.5	16.5	16.0	6.7
Ala	8.0	7.4	7.6	8.5
Val	5.0	4.0	3.7	4.3
Met	0	0.3	1.1	1.2
Ileu	3.2	4.2	3.0	1.8
Leu	5.3	6.1	6.5	14.6
Tyr	2.3	2.2	2.5	2.4
Phe	10.1	17.0	22.2	4.3
Lys	6.1	5.1	4.9	6.1
His	1.3	1.5	1.3	3.7
Arg	3.6	2.6	3.1	6.1

‡From Ref. 1

Table 9.2

SΔQ of the amino acid analyses of the basic proteins

	Cytosol	Lysosomes	Hepatocytes	L-subunit
Cytosol	0	-	-	-
Lysosomes	59	0	-	-
Hepatocytes	184	46	0	-
L-subunit	338	406	542	0

Since further experiments (effect of iron, polymerization, etc.) could not be carried out, it would be premature to state that the 40-kDa protein is a "building block" of ferritin. For the time being, all we can say is that it seems to be related to ferritin. Its exact origin, however, remains obscure.

MATERIALS & METHODS

See chapter 2

REFERENCES

1. **Crichton RR, Huebers H, Huebers E, Collet-cassart D, Ponce Y** (1975) Comparative studies on ferritin. In: Crichton RR (ed) Proteins of iron storage and transport in biochemistry and medicine. North Holland Publishing Company, Amsterdam, pp.193-200

CHAPTER 10

CONCLUSIONS

A great deal of research has been conducted into the relationship between ferritin and haemosiderin, the major iron-storing compounds in idiopathic haemochromatosis. Based on the results of these investigations, three hypotheses have been put forward:

I Haemosiderin is a degradation product of ferritin. Under iron-overload conditions, the amount of ferritin in the cytosol increases. As a result of changes at the surface of ferritin molecules, the molecules polymerize. Polymerization is a signal for incorporation into lysosomes. After incorporation, the polymers are degraded to insoluble haemosiderin.

II Haemosiderin is a degradation product of ferritin. This degradation takes place in siderosomes (iron-rich lysosomes). In the siderosomes the ferritin molecules lose their solubility and their protein coat is decomposed. The naked iron cores are disintegrated to haemosiderin.

III Haemosiderin iron has its origin in several sources and one of these sources is ferritin.

On the basis of the results presented in the previous chapters, we feel able to say that hypothesis I does not seem to be the most likely. The fact is that one would expect many polymers in the cytosolic fraction and these polymers should react less well to anti-(rat liver ferritin) antibodies, as a result of changes at their surface. In chapter 3, however, it is shown that the major fraction in the cytosol is the monomeric fraction, not the polymeric fraction (CVVF). Moreover, in chapter 4, we demonstrate that the CVVF fraction is recognized without problems by the anti-(rat liver ferritin) antibodies.
With reference to hypothesis II one would expect (1) siderosomal ferritin to be different from cytosolic and/or lysosomal ferritin and (2) in addition to ferritin and haemosiderin, intermediates to be present. This is exactly what we find. Chapter 5 shows that siderosomal ferritin differs morphologically from lysosomal and cytosolic ferritin: in the siderosomes the distance between the particles is less regular. After SDS treatment, its

protein coat dissociates into peptides of several sizes, whereas the other ferritins dissociate primarily into 20.5-kDa subunits. The siderosomal iron compound (SIC) can be regarded as an intermediate. On the one hand SIC is water-insoluble and morphologically resembles haemosiderin, on the other hand it contains (amongst other peptides) the 20.5-kDa ferritin subunit, which is recognized by anti-(rat liver ferritin) antibodies. The 20.5-kDa peptide in haemosiderin is no longer recognized. In short, we found much evidence to support hypothesis II.

However, there are a number of remarks to be added. Chapter 5 shows that all products that are present in the cytosolic fraction (CF, CLF and low-molecular-mass protein) are also present in the lysosomal fraction. This strongly indicates that the cytosolic products are incorporated in lysosomes without degradation.

CLF and the low-molecular-mass protein are further investigated. Chapter 8 shows that the presence of phosphorus or oxygen, but not the amount of iron per ferritin molecule, might provide an explanation for the difference in sedimentation rate between ferritin and light ferritin. Since the low-molecular-mass protein is present in cytosolic and lysosomal preparations, and never in siderosomal preparations, we expected it to be a "building block" of ferritin. However, chapter 9 shows that we can only conclude that it is related to ferritin. Its exact origin, however, remains obscure.

Results from chapter 6 emphasize that there is no relation between the amount of iron in the core and the core size. This means that differences in core diameters must be explained by alterations in the structure and compactness of the core. Based on the iron core measurements in chapter 5, this would mean that the ferritin core becomes less compact in lysosomes. Apparently, its structure becomes so loose that it eventually degenerates within siderosomes. The siderosomal iron compound can be regarded as disintegrated ferritin which still contains its epitopes. The cause of the change in structure is not clear. Perhaps the exchange of phosphorus (or oxygen) has something to do with it. As mentioned in chapter 5, ferritin iron itself could contribute to the degradation of ferritin in haemosiderin.

As the results in chapter 7 are meagre, we cannot comment on hypothesis III. However, hypothesis III does not contradict hypothesis II.

In conclusion, we can say that it is very likely that, in the experimental rat model, haemosiderin is a degradation product of ferritin. The degradation is preceded by storage in lysosomes. During storage, the structure of the ferritin iron core changes. The core becomes less compact, possibly due to exchange of phosphorus (or oxygen?) with its environment. Lysosomes become siderosomes as the storage process continues. In the siderosomes, the loosely packed ferritin core starts to disintegrate. Subsequently, iron particles from ferritin itself contribute to the degradation of ferritin into haemosiderin.

SUMMARY - SAMENVATTING

SUMMARY

Ferritin and haemosiderin are the major iron-storage compounds under iron-overload conditions. Ferritin is found in the cytosol and lysosomes/siderosomes (=iron rich lysosomes) of the cell, whereas haemosiderin is exclusively found in lysosomes/ siderosomes. Investigations into ferritin and haemosiderin revealed that they have much in common, but the iron particles in haemosiderin are smaller and they form aggregates due to an incomplete protein coat. There are a number of hypotheses about the transition process by which ferritin is degraded into haemosiderin, but it has still not definitively been established that all haemosiderin is derived from ferritin.
In this thesis we try to establish whether there is any relationship between ferritin and haemosiderin, and how any transition process might occur.
In chapter 3 the effect of dialysis on the iron/phosphorus (Fe/P) ratio of cytosolic and siderosomal ferritins is described. Prior to dialysis, both cytosolic and siderosomal ferritins were divided into monomers and polymers using gel filtration chromatography. The major fraction in the cytosol is the monomeric ferritin fraction (CMF). Its Fe/P ratio is not affected by dialysis. The major fraction in the siderosomes is the polymeric ferritin fraction (SVVF). This fraction contains only a trace of phosphorus, before and after dialysis. Purification with a KI gradient has no effect on the Fe/P ratio of haemosiderin. If haemosiderin is derived from ferritin, it must have taken up its phosphorus in siderosomes. In chapter 4 the morphology and mean iron-core diameter of the ferritin fractions isolated in chapter 3 are examined. Comparison of the mean iron-core diameter of CMF with SVVF shows that the mean iron-core diameter in the siderosomes is the larger. The results also show that the diameters of the individual iron particles that are present in the SVVF fraction, diverge more widely than those found in CMF.
In chapter 5 we adopt an alternative isolation scheme that enables us to isolate a cytosolic fraction, a lysosomal fraction and a siderosomal fraction in one single procedure. These three fractions are screened for iron-containing products. The products are isolated using ultracentrifugation. The cytosolic fraction contains a ferritin, a (slower sedimenting) light ferritin and an iron-free low-molecular-mass protein with ferritin epitopes. The lysosomal

fraction also contains these three products and, in addition, very little haemosiderin. The siderosomal fraction contains ferritin, a (faster sedimenting) iron-compound and haemosiderin. Analytical electron microscopy and SDS-PAGE indicate that real degradation of the ferritin molecule is confined to siderosomes.

In chapter 6 a pilot study is described in which we compare the cytosolic products formed after dietary (using carbonyl iron) and after parenteral (using iron dextran) iron-loading. Although dietary iron-loading is a slower process, similar products are formed in the cytosol, i.e. a ferritin (CF), a light ferritin (CLF) and a low-molecular-mass protein. There are no differences with respect to the protein coat. Analysis of the iron core shows that the two CF fractions are similar, whereas the two CLF fractions differ with respect to their iron content and to the packing of their cores. The carbonyl CLF product contains less Fe atoms per molecule, which, moreover, seem to be packed less compact.

With reference to the heterogeneity of the siderosomal fractions of chapters 3 and 4, the separation of parenchymal cells on the one hand, and sinusoidal cells on the other hand is described in chapter 7. Fractionation of parenchymal cells is successful, albeit with a very low yield. The fractionation of sinusoidal cells using digitonin does not succeed.

In chapter 8 cytosolic ferritins and light ferritins are compared. It is shown that the difference between these proteins cannot be explained by difference in iron content alone. Other elements in the core must also contribute to this. Their protein coats are similar. During a period of rest, in both fractions iron seem to be mobilized from the core without degradation of the molecule.

In chapter 9 the low-molecular-mass protein found in the cytosolic fraction of all our preparations is investigated. It proves to be a 40-kDa protein (*pI* about 8.6) which is recognized by anti-(rat liver ferritin) antibodies. Although it seems to be related to ferritin, its exact origin remains obscure, since it cannot be characterized completely.

In chapter 10 the hypothesis is put forward that, in an experimental rat model, cytosolic ferritin, after incorporation in lysosomes, undergoes changes in the structure of its core. The core becomes less compact. In siderosomes the core begins to disintegrate. Iron particles from the ferritin core itself play a role in the degradation of their own protein coat.

SAMENVATTING

Ferritine en hemosiderine zijn de belangrijkste ijzerstapelingsproducten in ijzerstapelingsziekten. Ferritine bevindt zich in het cytosol en in lysosomen/siderosomen (=ijzerrijke lysosomen), terwijl hemosiderine uitsluitend wordt aangetroffen in lysosomen/siderosomen. Onderzoek aan ferritine en hemosiderine heeft uitgewezen dat zij veel met elkaar gemeen hebben, maar dat de ijzerpartikels in hemosiderine kleiner zijn en aggregeren doordat hun eiwitmantel onvolledig is. Er bestaat een aantal hypothesen met betrekking tot het proces waarin ferritine wordt afgebroken tot hemosiderine. Het staat echter nog steeds niet definitief vast dat al het hemosiderine afkomstig is van ferritine. In dit proefschrift proberen we vast te stellen of er een verband is tussen ferritine en hemosiderine en hoe een eventueel omzettingsproces zou kunnen verlopen.

In hoofdstuk 3 wordt het effect van dialyse op de ijzer/fosfor (Fe/P) verhouding van ferritines uit het cytosol en uit de siderosomen beschreven. Vóór dialyse werden de ferritines uit het cytosol en uit de siderosomen met behulp van gelfiltratiechromatografie gescheiden in monomeren en polymeren. De voornaamste fractie in het cytosol is de monomere fractie (CMF). De Fe/P verhouding van deze fractie wordt niet beïnvloed door dialyse. De voornaamste fractie in de siderosomen is de polymere fractie (SVVF). Deze fractie bevat voor en na dialyse slechts een spoortje fosfor. Zuivering over een KI gradiënt heeft geen invloed op de Fe/P verhouding van hemosiderine. Als hemosiderine afkomstig is van ferritine, moet het in de siderosomen fosfor hebben opgenomen. In hoofdstuk 4 worden de morfologie en de gemiddelde diameter van de ijzerkernen van de ferritine fracties die in hoofdstuk 3 geïsoleerd zijn bestudeerd. Vergelijking van de gemiddelde ijzerkern diameter van CMF met die van SVVF laat zien dat de gemiddelde ijzerkern diameter in de siderosomen groter is. De resultaten laten tevens zien dat de diameters van de individuele ijzerpartikels in de SVVF fractie meer uiteenlopen dan die in de CMF fractie.

In hoofdstuk 5 schakelen we over op een ander isolatieschema dat ons in staat stelt in één procedure een cytosolfractie, een lysosomenfractie en een siderosomenfractie te isoleren. Deze drie fracties worden onderzocht op de aanwezigheid van ijzerbevattende producten.

De producten worden geïsoleerd met behulp van ultracentrifugatie. De cytosolfractie bevat een ferritine, een (langzamer sedimenterend) licht ferritine en een laagmoleculaire eiwitfractie zonder ijzer, maar met ferritine epitopen. De lysosomale fractie bevat eveneens deze drie producten en daarnaast nog een heel klein beetje hemosiderine. De siderosomale fractie bevat ferritine, een (sneller sedimenterende) ijzercomponent en hemosiderine. Analytische electronenmicroscopie en SDS-PAGE wijzen erop dat de echte afbraak van het ferritine molecuul alleen in de siderosomen plaatsvindt.
In hoofdstuk 6 wordt een voorstudie beschreven, waarin we de producten vergelijken die in het cytosol gevormd worden nadat ijzer oraal (carbonyl ijzer) en parenteraal (ijzer dextraan) is toegediend. Alhoewel ijzerstapeling na orale ijzertoediening een langzamer proces is, worden in het cytosol dezelfde producten gevormd: een ferritine (CF), een licht ferritine (CLF) en een laagmoleculaire eiwitfractie. Er zijn geen verschillen tussen beide eiwitmantels. Analyse van de ijzerkern laat zien dat de twee CF fracties hetzelfde zijn, terwijl de twee CLF fracties verschillen qua ijzergehalte en qua pakking van hun kern. Het carbonyl CLF product bevat minder Fe atomen per molecuul, die bovendien ook minder dicht gestapeld lijken te zijn.
In hoofdstuk 7 wordt, naar aanleiding van de heterogeniteit van de siderosomale fractie van hoofdstuk 3 en 4, de scheiding van de lever in parenchymcellen enerzijds en sinusoïdale cellen anderzijds beschreven. De fractionering van parenchymcellen lukt, zij het met een zeer lage opbrengst. De fractionering van de sinusoïdale cellen met behulp van digitonine lukt niet.
In hoofdstuk 8 worden het ferritine en het licht ferritine uit het cytosol vergeleken. Het blijkt dat het verschil tussen deze eiwitten niet alleen door een verschil in ijzergehalte verklaard kan worden. Ook andere elementen in de kern moeten hieraan bijdragen. Hun eiwitmantels zijn hetzelfde. Tijdens een rustperiode lijkt het er bij beide fracties op dat ijzer uit de kern gemobiliseerd wordt, zonder dat het molecuul wordt afgebroken.
In hoofdstuk 9 wordt de laagmoleculaire eiwitfractie die in al onze preparaten wordt aangetroffen, onderzocht. Het blijkt een eiwit van 40 kDa te zijn (p*I* ongeveer 8.6), dat herkend wordt door anti-(rattelever ferritine) antilichamen. Alhoewel het erop lijkt dat er een verband bestaat tussen het eiwit en ferritine, blijft de exacte oorsprong ervan

onduidelijk, daar het eiwit niet volledig gekarakteriseerd kan worden.
In hoofdstuk 10 wordt de hypothese naar voren gebracht dat, in een experimenteel rattemodel, ferritine uit het cytosol, na opname in lysosomen, veranderingen aan de structuur van zijn kern ondergaat. De kern wordt minder compact. In de siderosomen begint de kern uiteen te vallen. IJzerpartikels die afkomstig zijn van de ferritinekern zelf zouden een rol kunnen spelen in de afbraak van hun eigen eiwitmantel.

List of publications

The work described in this thesis is set down in the following papers and abstracts:

Papers:

Ringeling PL, Cleton MI, Kroos MJ, Sorber CWJ, de Bruijn WC, Harrison PM, van Eijk HG (1989) Lysosomal and cytosolic ferritins. A biochemical and electron-spectroscopic study. Biol Metals 2:114-121

Ringeling PL, Cleton MI, Huijskes-Heins MIE, Seip MJE, de Bruijn WC, van Eijk HG (1990) Analysis of iron-containing compounds in different compartments of the rat liver after iron loading. Biol Metals 3:176-182

Ringeling PL, Cleton, MI, Huijskes-Heins MIE, de Bruijn WC, van Eijk HG (1991) Comparison of cytosolic products formed in rat liver in response to parenteral and dietary iron-loading. Biol Trace Element Res (accepted)

Sorber CWJ, van Dort JB, Ringeling PL, Cleton-Soeteman MI, de Bruijn WC (1990) Quantitative energy-filtered image analysis in cytochemistry II. Ultramicroscopy 32,69-79

Ringeling PL, van Dun AJ, Huijskes-Heins MIE, Cleton MI, van Eijk HG Comparison of ferritins and light ferritins from rat liver cytosol. (in preparation)

Abstracts:

Ringeling PL, Kroos MJ, Cleton-Soeteman MI, de Jong AAW, de Bruijn WC, van Eijk HG (1988) The heterogeneity of liver ferritins. Meeting of the Dutch Association of Electron Microscopy, Rolduc, The Netherlands

List of publications

Ringeling PL, Kroos MJ, Cleton-Soeteman MI, de Jong AAW, de Bruijn WC, van Eijk HG (1989) The heterogeneity of liver ferritins. Proceedings of the 30th Dutch Federation Meeting, Maastricht, The Netherlands

Ringeling PL, Cleton-Soeteman MI, van Eijk HG (1989) Characterization of an iron-containing compound obtained during the isolation of ferritin from heavy lysosomes of iron-loaded rat livers. Iron Club Meeting, Budapest, Hungary

Ringeling PL, Cleton MI, de Bruijn WC, van Eijk HG (1989) Comparison of lysosomal and cytoplasmic iron-storage compounds from iron-loaded rat livers. Meeting of the Dutch Association of Electron Microscopy, Wageningen, The Netherlands

Ringeling PL, Cleton MI, de Bruijn WC, van Eijk HG (1990) Analysis of iron-containing compounds from iron-loaded rat livers using electron microscopy. Meeting of the Dutch Association of Electron Microscopy, Wageningen, The Netherlands

Ringeling PL, Cleton MI, Seip MJE, Huijskes-Heins MIE, de Bruijn WC, van Eijk HG (1990) Ferritins and ferritin-related compounds in cytosol, lysosomes and siderosomes from the rat liver after iron loading. European Iron Club Meeting, Porto, Portugal

Ringeling PL, Huijskes-Heins MIE, Cleton MI, de Bruijn WC, van Eijk HG (1991) Ferritins in rat liver after parenteral and dietary iron-loading. Proceedings of the 31st Dutch Federation Meeting, Amsterdam, The Netherlands

List of publications

Other publications:

Calafat J, Goldschmeding R, Ringeling PL, Janssen H, van der Schoot CE (1990) In situ localization by double-labeling immunoelectron microscopy of anti-neutrophil cytoplasmic autoantibodies in neutrophils and monocytes. Blood 75:242-250

van der Kraaij AMM, de Bruijn WC, Cleton MI, Ringeling PL, van Eijk HG, Essed NE, Koster JF. Specific iron-accumulation in myocardial endothelial cells and pericytes after short term iron-loading. Evidence for reperfusion injury to be initiated in vascular tissue (submitted)

CURRICULUM VITAE

Patricia Louise Ringeling werd geboren op 4 october 1964 te Amsterdam. In 1982 behaalde zij het Gymnasium α diploma aan het Sint Nicolaaslyceum te Amsterdam. In 1983 behaalde zij de VWO-deelcertificaten natuur- en scheikunde aan het avondcollege Contardo Ferrini te Amsterdam.
In hetzelfde jaar begon zij aan de studie scheikunde. Het doctoraalexamen scheikunde, met als hoofdvak biochemie en als bijvak immuno-electronenmicroscopie, werd in 1988 afgelegd aan de Universiteit van Amsterdam.
Van 1 mei 1988 tot 1 september 1991 was zij als wetenschappelijk medewerker werkzaam op de afdeling Chemische Pathologie van de Medische Faculteit van de Erasmus Universiteit Rotterdam. In deze periode werkte zij aan het in dit proefschrift beschreven onderzoek.